

**THERMAL AND MECHANICAL PROPERTIES OF LDPE/SISAL
FIBRE COMPOSITES COMPATIBILIZED WITH PARAFFIN WAXES**

by

**Lefu Piet Nhlapo (B.Sc. Hons.)
(2001130034)**

Submitted in accordance with the requirements for the degree

MASTER OF SCIENCE (M.Sc.)

Department of Chemistry

Faculty of Natural and Agricultural Sciences

at the

UNIVERSITY OF THE FREE STATE (QWAQWA CAMPUS)

SUPERVISOR: PROF A.S. LUYT

March 2010

Declaration

I declare that this thesis is my own independent work and has not been previously submitted at another university. I furthermore cede copyright of the dissertation in favour of the University of the Free State.

L.P. Nhlapo

Prof A.S. Luyt

Dedications

I dedicate this thesis to my lovely wife Mantshadi Nhlapo and blessed sons Katleho and Piet Nhlapo Junior for allowing me to be always excused among them for my M.Sc. degree studies. I wish to express my deepest gratitude to Masenuku Sarah Nhlapo (my grand mother), Motshidisi Jeannett Nhlapo (mother), Ngaka Nhlapo (uncle), Mathuso Nhlapo (aunt), Mamethe Lizzy Nhlapo (sister), Makiniri Daniel Nhlapo (younger brother) and Sebongile Patricia Nhlapo (sister) and all the relatives for the love and support during my studies.

Abstract

The effects of maleic anhydride grafted Fischer-Tropsch paraffin wax (MA-g-wax) and oxidised Fischer-Tropsch paraffin wax (OxWax) content on the morphology, thermal, mechanical and thermomechanical properties of LDPE/sisal fibre composites were examined in the current study. The composites and blends were prepared through melt mixing in a Brabender Plastograph internal mixer. Samples of different compositions were characterized for their morphology, thermal properties, mechanical properties and thermomechanical properties using scanning electron microscopy (SEM), differential scanning calorimetry (DSC), thermogravimetric analysis (TGA), tensile testing and dynamic mechanical analysis (DMA). Compatibility of the wax and the LDPE matrix is necessary as morphology has a significant effect on the composite properties. OxWax was partially miscible with LDPE at 5% wax content and co-crystallized with the LDPE matrix, but only partially miscible at 10% wax content. MA-g-wax, on the other hand, seemed to be more miscible with LDPE. TGA results showed an increase in the thermal stability in the presence of both waxes. In the presence of both 5 and 10% OxWax the tensile strength decreased at low sisal fibre contents (up to 15% fibre), but increased at higher fibre contents. The modulus increased in the presence of 5% OxWax and with increasing sisal fibre contents in the composites. However, the 5% OxWax containing composite samples showed higher moduli than the 10% OxWax containing composite samples as a result of co-crystallization of the wax and polymer at low wax content. The presence of MA-g-wax also increased the tensile strength of the composites. Elongation at break decreased with increasing fibre content in all cases. This indicated that the presence of fibre in the matrix reduced the ability of the sample to deform. The LDPE/MA-g-wax showed higher elongation at break values than the respective LDPE/OxWax blends. This is because MA-g-wax was more compatible with LDPE so that there was better interaction between the polymer and the wax and therefore better stress transfer. The OxWax, on the other hand, behaved differently due to the crystallization of the wax in the amorphous phase of the LDPE, and the crystals formed defect centres in the polymer matrix. The storage modulus generally increased with wax and fibre content. The MA-g-wax composite systems showed a shift in the β -transition indicating a better interaction between the LDPE and the fibres at higher fibre contents, which was not the case for the OxWax composite systems.

Table of contents

Contents	Page Number
DECLARATION	ii
DEDICATIONS	iii
ABSTRACT	iv
TABLE OF CONTENTS	v
LIST OF ABBREVIATIONS	vii
LIST OF TABLES	ix
LIST OF FIGURES	x
CHAPTER 1: General introduction	1
1.1 Background	1
1.2 Objective of the study	2
1.3 Thesis outline	3
1.4 References	3
CHAPTER 2: Literature review	5
2.1 Introduction	5
2.2 Polyolefin/wax blends	6
2.3 Natural fibre composites	7
2.3.1 Polyolefin/natural fibre composites	8
2.3.2 Thermal properties	11
2.3.3 Mechanical and thermomechanical properties	12
2.4 References	13
CHAPTER 3: Materials and methods	22
3.1 Materials	22
3.1.1 Waxes	22
3.1.2 Low density polyethylene	22
3.1.3 Maleic anhydride and dibenzoyl-peroxide	22

3.1.4	Sisal fibre	22
3.2	Methods	23
3.2.1	Preparation of maleic anhydride grafted Fischer-Tropsch wax (MA-g-wax)	23
3.2.2	Preparation of sisal fibres	23
3.2.3	Preparation of the blends and composites	24
3.2.4	Differential scanning calorimetry (DSC)	24
3.2.5	Thermogravimetric analysis (TGA)	25
3.2.6	Dynamic mechanical analysis (DMA)	25
3.2.7	Tensile testing	26
3.2.8	Scanning electron microscopy	27
3.3	References	28
CHAPTER 4:	Results and discussion	29
4.1	Scanning electron microscopy (SEM)	29
4.2	Differential scanning calorimetry (DSC)	31
4.3	Thermogravimetric analysis (TGA)	37
4.4	Tensile properties	39
4.5	Dynamic mechanical analysis (DMA)	45
4.6	References	53
CHAPTER 5:	Conclusions	56
5.1	Summary of observations	56
5.1.1	Uncompatibilized LDPE/sisal composites	56
5.1.2	LDPE/OxWax blends	56
5.1.3	LDPE/MA-g-wax blends	57
5.1.4	LDPE/sisal/OxWax composites	58
5.1.5	LDPE/sisal/MA-g-wax composites	58
5.2	Which wax is the best compatibilizer for the LDPE/sisal composites?	59
ACKNOWLEDGEMENTS		60
APPENDIX		61

List of abbreviations

ASTM	American Society for Testing and Materials
BF	Bamboo fibres
CRYSTAF	Crystallization analysis fractionation
ΔH_m^{obs}	Observed melting enthalpy
ΔH_m^{calc}	Calculated melting enthalpy
DBP	Dibenzoyl-peroxide
DMA/DMTA	Dynamic mechanical analysis/thermal analysis
DSC	Differential scanning calorimetry
EPR-g-MA	Ethylene-propylene rubber grafted with maleic anhydride
f-EPR	Functionalized ethylene propylene rubber
HCl	Hydrochloric acid
HDPE	High density polyethylene
HDPE-g-MA	High density polyethylene grafted with maleic anhydride
LDPE	Low-density polyethylene
LLDPE	Linear low-density polyethylene
LLDPE-g-MA	Linear low density polyethylene grafted with maleic anhydride
LMFI	Low melt flow index
MAH	Maleic anhydride
MA-g-wax	Maleic anhydride grafted Fischer-Tropsch wax
MAPE	Maleic anhydride grafted polyethylene
MFI	Melt flow index
MMFI	Medium melt flow index
nf-EPR	Non-functionalized ethylene-propylene rubber
NGOs	Non-governmental organizations
OxWax	Oxidized paraffin Fischer-Tropsch wax
PE	Polyethylene
PE-EPDM	Polyethylene/ethylene-propylene-diene terpolymer blend
PP	Polypropylene
PP-g-MA	Polypropylene grafted with maleic anhydride
SEM	Scanning electron microscopy

SEC-FTIR	Size exclusion chromatography - Fourier transform infrared spectroscopy
SMC	Unmodified methanol supercritical carbon dioxide cellulose
SMC-DC	Methanol supercritical carbon dioxide cellulose modified with dodecanoyl chloride
SMC-OC	Methanol supercritical carbon dioxide cellulose modified with octadecanoyl chloride
TGA	Thermogravimetric analysis
T _m	Melting temperature

List of tables

	Page
Table 3.1 Sample compositions used in this study	24
Table 4.1 Summary of DSC results for LDPE, LDPE/MA-g-wax and LDPE/OxWax blends, as well as LDPE/sisal, LDPE/sisal/ MA-g-wax and LDPE/sisal/OxWax composites	34
Table 4.2 Tensile testing data	40

List of figures

		Page
Figure 3.1	FTIR spectra for an unmodified Fischer-Tropsch wax and the same wax grafted with 5 wt% MAH	23
Figure 4.1	SEM micrographs for uncompatibilized 70/30 w/w LDPE/sisal composites 100x and 1000x magnifications	29
Figure 4.2	SEM micrographs for compatibilized 65/30/5 w/w LDPE/sisal/OxWax composites at 1000x, 20000x and 100x magnifications	30
Figure 4.3	SEM micrographs for compatibilized 65/30/5 w/w LDPE/sisal/MA-g-wax composites at 4800x, 20000x and 1000x magnifications	31
Figure 4.4	DSC heating curves of pure LDPE and LDPE/sisal fibre composites	32
Figure 4.5	DSC heating curves of pure LDPE and LDPE/OxWax blends	33
Figure 4.6	DSC heating curves of pure LDPE and LDPE/MA-g-wax blends	35
Figure 4.7	DSC heating curves of pure LDPE and LDPE/sisal/OxWax composites	36
Figure 4.8	DSC heating curves of pure LDPE and LDPE/sisal/Ma-g-wax composites	36
Figure 4.9	TGA curves of pure LDPE, OxWax, sisal, 90/10 w/w LDPE/OxWax blend and 60/30/10 w/w LDPE/sisal/OxWax composite	37
Figure 4.10	TGA curves of pure LDPE, MA-g-wax, sisal, 90/10 w/w LDPE/Ma-g-wax blend and 60/30/10 w/w LDPE/sisal/Ma-g-wax composite	39
Figure 4.11	Stress at break as function of sisal content for the LDPE/sisal/OxWax composites	41
Figure 4.12	Stress at break as function of sisal content for the LDPE/sisal/MA-g-wax composites	42
Figure 4.13	Elongation at break as a function of sisal content for the LDPE/	43

	sisal/OxWax composites	
Figure 4.14	Elongation at break as a function of sisal content for the LDPE/ sisal/MA-g-wax composites	43
Figure 4.15	Young's modulus as a function of sisal content for the LDPE/ sisal/OxWax composites	44
Figure 4.16	Young's modulus as a function of sisal content for the LDPE/ sisal/MA-g-wax composites	45
Figure 4.17	DMA storage modulus curves of pure LDPE, and untreated LDPE/ sisal composites	46
Figure 4.18	DMA loss modulus curves of pure LDPE and untreated LDPE/ sisal composites	47
Figure 4.19	DMA storage modulus curves of pure LDPE and LDPE/OxWax blends	48
Figure 4.20	DMA loss modulus curves of pure LDPE and LDPE/OxWax blend	49
Figure 4.21	DMA storage modulus curves of pure LDPE and LDPE/ MA-g-wax blends	50
Figure 4.22	DMA loss modulus curves of pure LDPE and LDPE/ MA-g-wax blends	50
Figure 4.23	DMA storage modulus curves of pure LDPE and LDPE/sisal/ OxWax composites	51
Figure 4.24	DMA loss modulus curves of pure LDPE and LDPE/sisal/ OxWax composites	51
Figure 4.25	DMA storage modulus curves of pure LDPE and LDPE/sisal /MA-g-wax composites	52
Figure 4.26	DMA loss modulus curves of pure LDPE and LDPE/sisal/ MA-g-wax composites	53

Chapter 1

General introduction

1.1 Background

The discovery of using cellulose fibre as reinforcement in composite materials is not a new or recent one. Man had used this idea for a long time, since the beginning of our civilization when grass and straw were used to reinforce clay and mud to make an adobe brick. This discovery was a major revolution, because the straw allowed the water to evaporate through uniformly distributed cracks in the clay. These greatly improved the strength of these early buildings [1]. During the seventies and eighties, cellulose fibres were gradually substituted by newly discovered synthetic fibres because of better performance. Plastic products contain fibreglass to give strength and toughness, reduce volume and/or reduce cost. Fibre-reinforced-plastic materials are considered as replacements for metals in situations where we need excellent specific strength properties, e.g. strength/weight and or stiffness/weight ratios [2]. Application of cellulose fibres came to a near halt, and the use of cellulose fibres was limited to the production of rope, string, clothing, carpets and other decorative products. In recent years, however, cellulose based fibres have been introduced as a possible replacement of synthetic fibres as reinforcement in plastic products [3].

It was a decade ago, in full recognition of global issues, that Greenpeace and other NGOs in various countries started to increasingly address the environmental impact of chemical substances. As a result of this awareness, governments were pushed towards more stringent legislation which promotes the preservation and protection of the quality of the environment for future generations. This, as well as high demands on materials having better overall performance has led to extensive research and development efforts in the composites fields [4]. Natural fibres are environment friendly materials, that are potentially user-friendly [5].

Unlike the typical engineering fibres, e.g. glass and carbon fibres, and mineral fillers, these lignocellulosic fibres are able to impart onto the composite certain benefits such as low density, less machine wear during processing, no health hazards, and a high degree of flexibility. These fibres, unlike the glass and carbon fibres, will bend rather than fracture

during processing. Whole natural fibres undergo some breakage while being intensively mixed with the polymeric matrix, but this is not as notorious as with brittle or man-made fibres [6,7]. Attempts were made to use natural fibre composites in place of glass mostly in non-structural applications. Therefore, attention has recently shifted to the fabrication and properties of natural fibre reinforced materials.

The automotive and aerospace industries both demonstrated an interest in using more natural fibre reinforced composites. For example, in order to reduce vehicle weight, automotive companies have already shifted from steel to aluminum and now are shifting from aluminum to fibre reinforced composites for some applications. This has led to predictions that in the near future polymer composites will comprise approximately 15% of the total automobile weight [8]. A significant number of automotive components, previously made from glass fibre composites, are now being manufactured using environmentally friendly composites [9,10]. For example, Daimler-Benz explored the idea of replacing glass fibre with natural fibre in automotive components since 1991, and Mercedes started using jute-based door panels in its E-class vehicles in 1996. This has now developed to such an extent that almost all the major German car manufactures use wood plastic composites in various applications [11,12]. Car manufacturers studied many materials and have used animal hair and fibres such as flax, sisal, coconut and cotton in upholstery, door panels and rear shelves of their cars. Local European renewable fibres, such as flax and hemp, are used for these cars. Ramie-fibres are examined too, because of their specific properties [13]. When a polymer (matrix) is combined with one or more materials (fillers) that are different in structure and morphology, the resultant product is called a polymer composite. Other applications of polymer composites are tractor fenders, decking and fencing materials, sewer pipes, car dashboards and septic tanks [14].

1.2 Objectives of the study

Polymers and polymer composites are widely used in modern society, and therefore it is the principal duty of all scientists to see that materials are developed that will not pollute the environment. One way is to synthesize bio-degradable polymers that will have the same properties as modern synthetic polymers. In the mean time polymer composites filled with natural fibre, because of the eco-friendliness of the fibre and because such composites are easier to recycle, may be used as alternatives to existing products. However, these composites have some inherent problems such as high water absorption and incompatibility with the

polymer matrices. These factors give rise to poor mechanical properties. One of the biggest challenges in this type of research is to improve the polymer-fibre compatibility in these composites, and to reduce their affinity for water. Hence, the purpose of this study was to investigate the possibility of using modified waxes as compatibilizers in sisal fibre reinforced polyethylene composites. This was achieved by melt-blending polyethylene with different amounts of sisal fibre, by investigating the morphology as well as the thermal and mechanical properties of the composites, and to try and explain the physical properties of the composites in terms of the observed morphologies.

1.3 Outline of the thesis

This manuscript comprises of five chapters.

Chapter 1: Background and objectives

Chapter 2: Literature survey

Chapter 3: Experimental

Chapter 4: Results and discussion

Chapter 5: Conclusions

1.4 References

1. <http://www.gogulftech.com/techform/default.htm#anchor1132163> (06/03/2006)
2. G. Kalaprasad, P. Pradeep, M. George, C. Pavithran, T. Sabu. Thermal conductivity and thermal diffusivity analyses of low-density polyethylene composites reinforced with sisal, glass and intimately mixed sisal/glass fibres. *Composites Science and Technology* 2000; 60:2967-2977.
3. M.A. Mokoena, V. Djoković, A.S Luyt. Composites of linear low density polyethylene and short sisal fibres: The effects of peroxide treatment. *Journal of Materials Science* 2004; 39:3403-3412.
4. P.T. Anastas, M.M. Kirchhoff. Origins, current status, and future challenges of green chemistry. *Accounts of Chemical Research* 2002; 35(9):686-694.
5. M. Idicula, S.K. Malhorta, K. Joseph, S. Thomas. Dynamic mechanical analysis of randomly oriented intimately mixed short banana/sisal hybrid fibre reinforced polyester composites. *Composites Science and Technology* 2005; 65:1077-1087.

6. Y. Mi, X. Chen, Q. Guo. Bamboo fiber-reinforced polypropylene composites: crystallization and interfacial morphology. *Journal of Applied Polymer Science* 1997; 64:1267-1273.
7. Y. Li, C. Hu, Y. Yu. Interfacial studies of sisal fibre reinforced high density polyethylene (HDPE) composites. *Composites Part A* 2008; 39:570-578.
8. A.K. Mohanty, L.T. Drzal, M. Misra. Novel hybrid coupling agent as an adhesion promoter in natural fiber reinforced powder polypropylene composites. *Journal of Materials Science Letters* 2002; 21:1885-1888.
9. H. Larbig, H. Scherzer, B. Dahlke, R. Poltrock. Natural fibre reinforced foams based on renewable resources for automotive interior applications. *Journal of Cellular Plastics* 1998; 34:361-379.
10. F.G. Torres, M.L. Cubillas. Study of the interfacial properties of natural fibre reinforced polypropylene. *Polymer Testing* 2005; 24:694-698.
11. M. Jacob, T. Sabu. Biofibres and biocomposites. *Carbohydrate Polymers* (in press).
12. A. Bismack, A. Baltazar-Y-Jimenez, K. Sarlkakiy. Green composites as Panacea? Socio-economic aspects of green materials. *Environment, Development and Sustainability* 2006; 8:445-463.
13. A.K. Bledzki, J. Gassan. Composites reinforced with cellulose based fibers. *Progress in Polymer Science* 1999; 24:221-274.
14. P. Augustine, J. Kuruvilla, T. Sabu. Effect of surface treatments on the electrical properties of low-density polyethylene composites reinforced with short sisal fibers. *Composites Science and Technology* 1997; 57:67-79.

Chapter 2

Literature review

2.1 Introduction

A composite material is generally a material composed of a mixture or combination of two or more micro- or macro constituents with an interface separating them that differs in form and chemical composition, and that are essentially insoluble in each other. The primary purpose for making these materials is that superior or important properties compared to that of the individual components could be achieved.

The incorporation of natural fibres into a polymer commonly leads to substantial changes in the mechanical properties of the composites. However, a problem encountered when trying to combine natural fibres with thermoplastic materials like polyolefins is one of incompatibility due to the hydrophilic nature of the natural fibres. Therefore, the use of a compatibilizer or coupling agent, which alleviates gross segregation and promotes adhesion, is necessary to reduce the interfacial tension between the hydrophobic polyolefins and the hydrophilic natural fibres. The choice of compatibilizers or coupling agents is critical for optimizing the dispersion and properties of the polyolefins. Besides, a good compatibilizer should provide stronger adhesion between the natural fibres and form entanglement and/or segmental crystallization with the polymeric matrix. The polymeric compatibilizer is expected to be miscible with the matrix material as morphology has a significant effect on the polymer properties.

Blending paraffin waxes with polyethylenes normally provides a polymeric material with improved processability, because oxidized paraffin wax and maleic anhydride grafted wax is miscible with polyethylenes, and they may therefore improve the interaction between the hydrophobic polyethylene and the hydrophilic sisal fibres.

2.2 Polyolefin/wax blends

The thermal and mechanical behaviour of polyolefin/wax blends is a subject which has been well documented by Luyt and coworkers [1-13]. Their studies concentrated on the relationship between blend morphology, processing conditions and physical properties. There is almost no other literature on this topic.

Krupa and Luyt [1] investigated the thermal and mechanical properties of linear low-density polyethylene (LLDPE) mixed with a hard paraffin wax. They prepared the blends using an industrial extruder. The DSC heating curves showed one endothermic peak for 10 and 20% wax content due to the miscibility of LLDPE and wax in the crystalline phase. However, at 30 % and higher wax contents, three significant peaks were observed. This meant that at these concentrations LLDPE and wax were not completely miscible in the crystalline phase. The tensile testing results showed an increase in Young's modulus with an increase in wax content due to the higher crystallinity of the material. A decrease in elongation at break with an increase in wax content was also observed at all the investigated wax contents.

Djoković *et al.* [5] studied the effect of oxidized Fischer-Tropsch paraffin wax on the thermal, mechanical and viscoelastic properties of low-density polyethylene (LDPE)/wax blends. These blends were prepared using an industrial extruder. The DSC results showed that the blends had similar melting behaviour to that of pure LDPE as a result of co-crystallization up to 20% wax content. However, at 30% and higher wax contents, another melting peak appeared at lower temperatures, which was due to LDPE and wax crystal separation.

Krupa and Luyt [6] studied the influence of oxidized paraffin waxes on the physical properties of LLDPE. The blends were mechanically mixed using a coffee mill. Only one endothermic peak was observed at all the investigated compositions, despite the fact that pure wax showed two significant peaks at lower temperatures. Similar results were reported by Luyt and Geethamma [7] and by Luyt and Brüll [8]. They suggested that LLDPE and wax were miscible in the crystalline phase. A decrease in thermal stability of the blends with an increase in wax content was observed due to the much lower thermal stability of the wax compared to that of the LLDPE. The tensile testing results showed an increase in Young's modulus with an increase in wax content due to the higher modulus of the wax.

Krupa *et al.* [11] investigated the influence of soft and hard paraffin waxes on the properties of isotactic polypropylene (PP). They prepared the blends through melt mixing followed by compression moulding. The DSC results showed two pronounced separated peaks for both hard and the soft wax due to a solid-solid transition and melting of the crystallites. There was a decrease in the melting point of PP with an increase in wax content due to the plasticization of the PP by the wax. Hato and Luyt [13] investigated the influence of hard and oxidized paraffin wax on the properties of their blends with HDPE, LDPE and LLDPE. They prepared blends using melt mixing followed by melt pressing. The DSC results showed complete miscibility when HDPE was blended with 10 and 20 wt% of both waxes. The LDPE blends showed one endothermic peak for only 10% of both waxes. The LLDPE blended with the oxidized wax gave rise to complete miscibility at all the investigated compositions, which was not the case for the hard paraffin wax containing blends.

2.3 Natural fibre composites

Natural fibres have been extensively investigated by both scientists and engineers as reinforcements in polyolefins [12-19]. The growing interest in using natural fibres as a reinforcement of polymeric based composites is mainly due to their abundant, renewable origin, relatively high specific strength and modulus, light weight and biodegradability [20]. Natural fibres are also called ‘plant fibres’, ‘cellulose fibres’ or ‘vegetable fibres’. They are lignocellulosic consisting of helically wound cellulose microfibrils in an amorphous matrix of lignin and hemicellulose. These cellulose fibres/fillers include banana (*musa sepientum*), coir (*cocus nicifera*), cotton (*gossypium M.*), curauá (*ananas erectofolius*), flax (*linum usitatisimum*), hemp (*cannabis sativa*), jute (*carchorus capsularis*), kenaf (*hibiscus cannabinus*), mesta (*hibiscus sibdoriff*), paina (*chorisia speciosa*), paíçava (*attalea funifera*), pineapple (*ananas comosus*), ramie (*boehmeria nivea*), sisal (*agave sisalana*), sponge-gourd (*laffa cylindrical*) and sun hemp (*crotolavia juncea*) [21]. In addition to the fibres already mentioned, many other lignocellulosic materials were discussed in the available literature, and they may be used in various applications, but particularly in the development of composite materials. The major ones are abaca, alfa, bagasse, bamboo, henequen, kapok, kraft, kraut, palm, sago, skew pine, aot and wood fibre [2,16,21]. These fibres are generally extracted from pseudo-stem, mesocarp, leaf sheats and stalks using machine-decorticators, and primitive machines such as ‘periquita’ and forca [21].

Cellulose is the primary component of natural fibres. It is a linear condensation polymer consisting of *D*-anhydro-glucopyranose units joined together by β -1,4-glucosidic bonds [12,17,21]. The mechanical properties of the natural fibres are dependent on the cellulose content in the fibre, the degree of polymerization of the cellulose and the microfibril angle [22]. The natural fibres can be grouped into bast, leaf and seed or fruit, depending on their origin, and they therefore possess varying cellulose content. Singleton *et al.* [17] and Herrera-Franco *et al.* [20] reported that henequen and flax, which are extracted from the bast, have 60% cellulose content. Joseph *et al.* [22] reported that sisal fibres (extracted from the leaves) consist of 85-88% cellulose content.

Natural fibres possess desirable properties such as high specific strength, light weight, ease of separation, enhanced energy recovery, high toughness, non-corrosive nature, low density, low cost, good thermal properties, reduced tool wear, reduced dermal and respiratory irritation, less abrasion of processing instruments, as well as recyclability and biodegradability [23-29]. However, the majority of cellulose fibres have low degradation temperatures (~ 200 °C), which make them inadequate for processing with thermoplastics above 200 °C. Their high moisture uptake and their tendency to form aggregates during processing, represent some of the drawbacks related to their use in cellulose fibre composites. The behaviour and properties of these fibres depend on many factors such as harvest period, weather variability, and quality of soil and climate of the specific geographical location [30-31]. Recent developments showed that it is possible to improve the mechanical properties of cellulose fibre-reinforced composites by chemical modification that may promote good adhesion between the polyolefins and the fibres.

2.3.1 Polyolefin/natural fibre composites

Different techniques have been used to prepare polyolefin/natural fibre composites. These techniques/methods include solution mixing, roll milling, melt mixing, as well as injection and compression moulding [32-43]. The methods differ in terms of their operating principles and processing parameters, which may lead to fairly different properties of the prepared composite materials. Polyolefin/natural fibre composites were generally pretreated on the surface of the fibre or incorporated with surface modifiers to improve the interfacial adhesion between the hydrophilic natural fibres and the hydrophobic polyolefins. This can be achieved by using treatments such as silane coupling agents, compatibilizers, maleated polyolefins

(maleic anhydride grafted polypropylene or maleic anhydride grafted polyethylene), as well as alkali and radiation treatments [32,33,39,46].

Many studies focused on the preparation and morphology of non-treated composites. Colom *et al.* [38] and Mengeloglu *et al.* [47] focused on non-treated HDPE/wood fibre composites. The composites were prepared using a Brabender roll mill and a single screw extruder. They used scanning electron microscopy (SEM) to identify the morphologies of their samples. They found poor adhesion between the non-polar HDPE matrix and the polar wood fibre, and inadequate wetting of the non-treated fibres within the HDPE matrix. They related these to the presence of large numbers of voids between the HDPE matrix and the wood fibre, and fibre-pull-out producing holes with smooth walls in the polymer matrix. The SEM results, in all cases, showed that non-treated fibres appeared to be free of any matrix adhering to them [36]. However, Li *et al.* [48] and Bengston *et al.* [49] reported that some parts of the wood fibre were covered with the polymer due to mechanical interlocking. Herrera-Franco *et al.* [44], Albano *et al.* [36] and Mohanty *et al.* [43] investigated composites based on HDPE and henequen fibre, seaweed residues and jute fibres. These composites were prepared using roll milling, compression moulding and melt mixing. The SEM results revealed poor interfacial adhesion between the components in the non-treated composites due to poor interfacial adhesion.

LDPE was also reinforced with natural fibres and the composites characterized for their morphology. Torres *et al.* [45] and Joseph *et al.* [50] used sisal fibre, whereas Kaci *et al.* [51] used oil husk flour to reinforce LDPE. The composites were prepared through compression moulding, melt mixing and solution mixing. The SEM results for all the studies showed relatively large gaps, fibre pull out and no coating on the surface of the fibres. Oksman *et al.* [52] and Freire *et al.* [53] used wood fibres to reinforce an LDPE matrix. In both cases the composites were prepared through injection moulding. Again the SEM results in all cases showed poor interfacial adhesion between the wood fibre and the LDPE matrix.

LLDPE was also filled with natural fibres and characterized for their morphology. Marcovich *et al.* [53] and Kuan *et al.* [54] used wood fibre, while Kim *et al.* [55] used saw dust to reinforce LLDPE. A counter rotating twin screw extruder [53], a co-rotating twin-screw extruder [54], and melt blending [55] were used for the preparation of these composites. In all

the cases the SEM results showed distinct gaps between the cellulose and the matrix, indicating poor interfacial adhesion.

PP/natural fibre composites were extensively investigated by various researchers. Nachtigall *et al.* [56], Nygård *et al.* [57], Albano *et al.* [33] and Yuan *et al.* [58] used wood fibre to reinforce the PP matrices. The PP/wood fibre composites were prepared through melt mixing [33,56] and twin screw extrusion [57,58]. The SEM results showed many voids, cavities [56] and fibre pull-out [33,58]. Nygård *et al.* [57], however, in their study of PP/wood fibre composites observed no difference between the treated and untreated PP/wood fibre composites. For all the composites a rough and porous structure was observed because of poor fibre dispersion for the untreated composites. Mohanty *et al.* [59], Fung *et al.* [60] and Joseph *et al.* [14,15] used sisal fibre to fill PP matrices. The samples were prepared through twin-screw extrusion [59,60] and melt mixing [14,15]. The SEM results in all the cases revealed a fairly efficient dispersion with few unwetted fibres, gaps and extensive fibre pull-outs. Pracella *et al.* [61] and Beckermann *et al.* [62] used hemp fibre to reinforce polypropylene matrices. The composites in these cases were prepared through internal mixing and extrusion. The SEM results showed poor interaction between the fibre and the matrix with debonding of the fibres in all the cases.

Coupled polyolefin/natural fibre composites showed improved properties related to the morphology. The coupling was done on either the fibre surface or through polymer treatment. These provided enhanced interfacial adhesion between the polymer matrix and the fibre, good fibre dispersion within the matrix and good fibre coating by the polymer. The degree of interfacial adhesion of the composite components was shown to depend largely on the chemical nature of the chosen coupling agent [63]. Various coupling agents such as wax, silane, organosilanes, maleic anhydride, maleic anhydride grafted polyolefins, acrylic acid grafted polyolefins, organic peroxides, ethylene-vinyl alcohol copolymers, and poly(ethylene-co-vinyl acetate) were used to enhance the compatibility between the natural fibres and the polyolefins [14,15,33,56-62]. Through the application of these coupling agents good compatibility and interfacial adhesion between the polyolefin matrices and the various natural fibres were achieved. All the SEM results generally showed the absence of gaps between the fibres and the matrices, reduction in fibre pull-outs resulting in small voids and few cavities, improved fibres dispersion within the polymer matrices, good fibre covering by the polymers and less fibre agglomeration.

2.3.2 Thermal properties

The investigations on the thermal properties of the polyolefin/natural fibre composites were generally conducted by comparing the degradation behaviour of natural fibre, virgin polyolefin, and untreated polyolefin/natural fibre composites compared to the treated composites. In most cases the treated composites showed higher thermal stability than both the untreated composites and the pure components [36,56,59,62-67]. However, Pickering *et al.* [62] observed higher thermal stability for the untreated PP/hemp composites than the treated composites where MAPP was used as a coupling agent.

Sarkhel and Choudhury [64] investigated the thermal properties of ternary composites based on a low-density polyethylene (LDPE)-ethylene-propylene-diene terpolymer (EPDM) blend and high density polyethylene (HDPE)-EPDM blends reinforced with short jute fibres. The DSC results showed a decrease in T_m of the LDPE and HDPE components for both untreated and treated composites, although, this trend decreased with an increase in fibre loading and MAPE dose. Viksne *et al.* [65] investigated the effect of paraffin wax as a dispersing agent to reduce agglomeration of wood fibre in different polyolefin (LDPE, HDPE, and recycled LDPE) matrices. The composites were prepared using a two-roll mill, compression moulding and injection moulding. The DSC results showed segregation of the material. Two melting peaks were observed in all composite systems investigated. They associated this behaviour with the immiscibility between the paraffin wax used and the polyethylene matrix.

Doh *et al.* [66] used TGA and DSC to investigate the thermal behaviour of different polyolefin (LDPE, HDPE and PP) matrices reinforced with liquefied wood. The composites were prepared through injection moulding. The effects of the temperature, heating rate, polymer type, melt index, and liquefied wood level (0-40%) on the thermal behaviour were investigated. There was generally no significant influence on the thermal behaviour of all the samples at 10% liquefied wood content. All the composites showed poor thermal stability with increasing liquefied wood content due to poor compatibility and interfacial adhesion between the polyolefin and liquefied wood. At higher heating rates, better thermal stability resulting from decelerated decomposition rates was observed. The DSC results showed a decrease in T_m of all the composites investigated at 10% liquefied wood content, while the enthalpy of melting of the polymer decreased with increasing liquefied wood content. Pasquini *et al.* [67] reported a different observation in their investigation of the thermal

properties of low-density polyethylene/cellulose fibre composites. They directly linked T_m to the crystalline domain size of the LDPE film and assumed that to be influenced by the presence of filler. They observed no general influence on T_m for all the systems (modified organosolv/methanol-supercritical carbon dioxide cellulose (SMC) and modified octadecanoyl chloride-SMC or dodecanoyl chloride) investigated, even though a decrease in the enthalpy of melting with an increase in filler content was observed due to a decrease in the fraction of matrix material. The tensile results showed an increase in Young's modulus with an increase in filler content. By adding unmodified SMC into LDPE, a considerable reduction in the tensile strength was observed, whereas for the modified SMC-DC and SMC-OC cellulose based composites the observed reduction in the tensile strength was less pronounced due to better interfacial adhesion, and an improved level of fibre dispersion in the matrix. A dramatic decrease in elongation at break with an increase in fibre content was also observed. They related this behaviour to the actual elongation experienced by the polymeric matrix, which was much higher than that measured for the sample itself.

2.3.3 Mechanical and thermomechanical properties

The incorporation of natural fibres into a polymer is known to cause substantial changes in the mechanical properties of the composites. The quality of the fibre-matrix interface is important for the application of natural fibres as reinforcement for polymers. Since the fibres and matrices are chemically different, strong adhesion at their interfaces is needed for an effective stress transfer and bond distribution throughout the interface. The term “interface” has generally been defined as the boundary region between two phases in contact. The mechanism of reinforcement is dependent on the stress transfer between the matrix material and the embedded fibre. In particular, the fibre-matrix interfacial shear strength is one of the most important parameters in controlling the toughness and the strength of a composite material. Its value is particularly dependent on fibre surface treatment, modification of the matrix and other factors affecting the properties of the fibre-matrix interface [18,24,49,68,69]. A number of studies reported on the effect of poor or good interfacial adhesion on the mechanical and viscoelastic properties of the polyolefin/natural fibre composite materials.

Mohanty *et al.* [43] investigated HDPE/jute composites with different maleic anhydride grafted polyethylene contents. The composites were prepared using compression moulding. An improvement in the mechanical properties of the untreated composites was observed, due

to the reinforcing effect imparted by the fibres which allowed a uniform stress distribution from the continuous polymer matrix to the dispersed fibre phase. However, there was a general improvement in the mechanical properties of the treated composites in comparison to those of the untreated composites. The DMA results showed that the incorporation of jute fibres into HDPE increased the modulus due to the increase in stiffness of the matrix with the reinforcing effect imparted by the fibres that allowed a greater degree of stress transfer at the interface. A broadening of the PE peak transition region was observed for both untreated and treated composites due to inhibition of the relaxation process within the composites with the addition of fibres. This is in agreement with observations by Lai *et al.* [70], who investigated the effect of maleated polyolefins (PP-g-MA, HDPE-g-MA and LLDPE-G-MA) on the mechanical properties of HDPE/wood flour composites. The composites were prepared using a self-wiping co-rotating twin-screw extruder. They observed a general improvement in the tensile strength of the compatibilized composites with respect to the unmodified system. An increase in the storage modulus with the addition of fibre was observed, and a further increase was observed in the presence of the compatibilizers at the transition and plateau regions, except where PP-g-MA was used as compatibilizer, where little difference from the untreated system was observed. A $\tan \delta$ broadening and a peak shift were observed due to the interaction between the polymer matrix and the filler.

Lui *et al.* [71] investigated HDPE/bamboo fibre (BF) composites with two maleated ethylene/propylene elastomers (EPR-g-MA) and a maleic anhydride grafted polyethylene as compatibilizers. They prepared the composites using a counter-rotating twin-screw extruder. Their tensile testing results show a decrease in tensile strength for the untreated composite systems compared to the virgin PP due to poor interfacial adhesion. However, by adding EPR-g-MA or PE-g-MA, an increase in the tensile strength was observed due to improved interfacial adhesion. They suggested that the applied load was transferred through the interface between the HDPE matrix and the rigid BF. The DMA results showed that the storage modulus increased remarkably with the addition of BF into HDPE due to enhanced stiffness, despite the fact that the untreated composites showed a higher storage modulus than the treated composites. The dynamic loss modulus also increased with increasing BF content. A shift of the α -relaxation peak of the composites to higher temperatures compared to that of the virgin HDPE was observed. However, this was not the case with the EPR-g-MA treated composites where no change in the α -relaxation position was observed. The highest α -relaxation peak was observed for PE-g-MA modified composites due to the strong restriction

effect on the relaxation behaviour. The presence of PE-g-MA in the composite showed increased loss factor ($\tan \delta$) values compared to the pure HDPE. The authors associated this observation as an inhibition effect of the fibres on the relaxation process.

Different trends were observed by Ichazo *et al.* [72] who investigated the composite systems of PP, PP/HDPE, PP/HDPE/functionalized (f) ethylene-propylene rubber and PP/HDPE/non-functionalized (nf) ethylene-propylene rubber reinforced with sisal fibres. The composites were prepared in one stage using a co-rotating twin screw extruder. There was an increase in tensile strength with increasing fibre content. Acetylated treatment improved the tensile modulus with about 40% compared to that of pure PP. Similarly, the tensile test results showed an increase of about 35% in the tensile modulus of untreated polyolefin (PP, PP/HDPE, PP/HDPE/f-EPR and PP/HDPE/nf-EPR)/sisal fibre composites. Irrespective of the acetylation of the fibres, sisal fibre is able to impart greater stiffness to polyolefin composites. A decrease in elongation at break was observed for all the composites with treated and untreated sisal fibres due to a reduction in deformability of the rigid interface between the fibre and the matrix components, which was reflected in an increase in the stiffness.

Balasuriya *et al.* [73] investigated the structure-property relationships of wood flake-HDPE composites, and no coupling agent or compatibilizer was used. They compared the effect of different compounding techniques on the mechanical properties of the composites. The composites were prepared using twin-screw compounding on a medium melt flow index (MMFI) polymer, and low melt flow index (LMFI) polymer. There was a general decrease in tensile strength with increasing wood flakes content due to the poor interfacial adhesion between the hydrophilic wood flakes and the hydrophobic HDPE. However, the tensile strength increased for composites prepared through MMFI from 10 to 20 wt% wood flakes content. They suggested the improved flake wetting, dispersion and PE penetration into some of the lumens of the wood fibres were the root causes of this behaviour. This mechanism was believed to be the same for tensile modulus, flexural modulus, and ultimate elongation at yield or break, even though no yield was observed for composites containing more than 40 wt% wood flakes.

Pasquini *et al.* [67] studied LDPE/sugar cane bagasse with modified organosolv/methanol-supercritical carbon dioxide cellulose (SMC) and modified octadecanoyl chloride-SMC (SMC-OC) or dodecanoyl chloride (SMC-DC). They used melt mixing followed by hot

pressing at 150 °C. Their DMA results showed an increase in storage modulus with increasing fibre content due to the reinforcing effect of the cellulose fibres, which increased the rubbery modulus of the LDPE. This effect was higher for unmodified SMC than for the modified fibre (SMC-DC, SMC-OC). They suggested the degradation of the cellulose molecules during the surface modification process to be the root cause as observed from degree of polymerization measurements. There was an increase in Young's modulus with an increase in filler content. By adding unmodified SMC in LDPE, a considerable reduction in the tensile strength was observed, whereas for modified SMC-DC and SMC-OC cellulose based composites the reduction in the tensile strength was less pronounced due to better interfacial adhesion and an improved level of fibre dispersion in the matrix. A dramatic decrease in elongation at break with an increase in fibre content was observed due to the fact that the actual elongation experienced by the polymeric matrix is much higher than that measured for the sample itself. Rahman *et al.* [74] investigated the influence of benzene diazonium on PP and abaca fibre composites. Composites of different fibre content (10, 15, 20 and 25%) were prepared through a single screw extruder. There was a decrease in the tensile strength of the untreated composites with an increase in fibre content. This is due to the increase in the micro spaces between the filler and the matrix with increasing filler content, which weakens the filler-matrix adhesion. However, an increase in tensile strength of the treated composites at all compositions was observed due to improved interfacial adhesion between the filler and the matrix. An increase in Young's modulus with increasing filler content for both treated and untreated abaca fibre was observed, but higher moduli were observed for treated composites compared to untreated composites. It was suggested that a reduced chain matrix mobility with the incorporation of the fibre led to the stiffness of the composites.

2.4 References

1. I. Krupa, A.S. Luyt. Thermal and mechanical properties of extruded LLDPE/wax blends. *Polymer Degradation and Stability* 2001; 73:151-161.
2. I. Krupa, A.S. Luyt. Thermal properties of uncrosslinked and crosslinked LLDPE/wax blends. *Polymer Degradation and Stability* 2000; 70:111-117.
3. F.M. Mhlongo, A.S. Luyt. C.G.C.E. Van Sittert. Effect of cross-linking on the thermal stability and molar mass distribution of paraffin waxes. *Polymer Degradation and Stability* 2001; 73:151-155.

4. M.J. Hato, A.S. Luyt. Thermal fractionation and properties of different polyethylene/wax blends. *Journal of Applied Polymer Science* 2007; 104:2225-2236.
5. S.P. Hlangothi, I. Krupa, V. Djoković, A.S. Luyt. Thermal and mechanical properties of crosslinked and uncrosslinked linear low-density polyethylene-wax blends. *Polymer Degradation and Stability* 2003; 79:53-59.
6. V. Djoković, T.N. Mtshali, A.S. Luyt. The influence of wax content on the physical properties of low-density polyethylene-wax blends. *Polymer International* 2003; 52:999-1004.
7. I. Krupa, A.S. Luyt. Physical properties of blends of LLDPE and an oxidized paraffin wax. *Polymer* 2001; 42:7285-7289.
8. A.S. Luyt, V.G. Geethamma. Effect of oxidized paraffin wax on the thermal and mechanical properties of linear low-density polyethylene-layered silicate nanocomposites. *Polymer Testing* 2007; 26:461-470.
9. A.S. Luyt, R. Brüll. Investigation of polyethylene-wax blends by CRYSTAF and SEC-FTIR. *Polymer Bulletin* 2004; 52:177-183.
10. H.S. Mpanza, A.S. Luyt. Comparison of different waxes as processing agents for low-density polyethylene. *Polymer Testing* 2006; 25:436-442.
11. T.N. Mtshali, I. Krupa, A.S. Luyt. The effect of crosslinking on the thermal properties of LDPE/wax blends. *Thermochimica Acta* 2001; 380:47-54.
12. I. Krupa, A.S. Luyt. Thermal properties of polypropylene/wax blends. *Thermochimica Acta* 2001; 372:137-141.
13. I. Novák, I. Krupa, A.S. Luyt. Modification of the polarity and adhesive properties of polyolefins through blending with maleic anhydride grafted Fischer-Tropsch paraffin wax. *Journal of Applied Polymer Science* 2006; 100:3069-3074.
14. M.J. Hato, A.S. Luyt. Thermal fractionation and properties of different polyethylene/wax blends. *Journal of Applied Polymer Science* 2007; 104:2225-2236.
15. Y. Li, Y-W. Mai, L. Ye. Sisal fibre and its composites: a review of recent developments. *Composites Science and Technology* 2000; 60:2037-2055.
16. A. Paul, K. Joseph, S. Thomas. Effect of surface treatments on the electrical properties of low-density polyethylene composites reinforced with short sisal fibers. *Composites Science and Technology* 1997; 57:67-79.
17. P.V. Joseph, K. Joseph, S. Thomas, C.K.S. Pillai, V.S. Prasad, G. Groeninckx, M. Sarkissova. The thermal and crystallization studies of short sisal fibre reinforced polypropylene composites. *Composites Part A* 2003; 34:253-266.

18. P.V. Joseph, M.S. Rabello, L.H.C. Mattoso, K. Joseph, S. Thomas. Environmental effects on the degradation behaviour of sisal fibre reinforced polypropylene composites. *Composites Science and Technology* 2002; 62:1357-1372.
19. T. Aurich, G. Mennig. Determination of interfacial shear strength and critical fibre length in injection moulded flax fibre reinforced polypropylene. *Advanced Composites Letters* 2001; 10(6):299-303.
20. A.C.N. Singleton, C.A. Baillie, P.W.R. Beaumont, T. Peijs. On the mechanical properties, deformation and fracture of a natural fibre/recycled polymer composites. *Composites Part B* 2003; 34:519-526.
21. C. Albano, J. González, M. Ichazo, D. Kaiser. Thermal stability of blends of polyolefins and sisal fiber. *Polymer Degradation and Stability* 1999; 66:179-190.
22. M.Q. Zhang, M.Z. Rong, X. Lu. Fully biodegradable natural fiber composites from renewable resources: all plant fiber composites. *Composites Science and Technology* 2005; 65:2514-2525.
23. P.J. Herrera-Franco, A. Valadez-González. A study of the mechanical properties of short natural-fiber reinforced composites. *Composites Part B* 2005; 36:597-608.
24. D.G. Dikobe, A.S. Luyt. Effect of poly(ethylene-co-glycidil methacrylate) compatibilizer content on the morphology and physical properties of ethylene vinyl acetate-wood fiber composites. *Journal of Applied Polymer Science* 2007; 104:3206-3213.
25. T.H.D. Syndenstricker, S. Mochnaz, S.C. Amico. Pull-out and other evaluations in sisal-reinforced polyester biocomposites. *Polymer Testing* 2003; 22:375-380.
26. K. Jayaraman, Manufacturing sisal-polypropylene composites with minimum fibre degradation. *Composites Science and Technology* 2003; 63:367-374.
27. K. Joseph, S. Thomas, C. Pavithran. Effect of chemical treatment on the tensile properties of short sisal fibre reinforced polyethylene composites. *Polymer* 1996; 37:5139-5149.
28. J. Kuruvilla, T. Sabu, C. Pavithran. Effect of ageing on the physical and mechanical properties of sisal-fibre reinforced polyethylene composites. *Composites Science and Technology* 1995; 53:99-110.
29. M. Jacob, S. Thomas, K.T. Vuraghese. Mechanical properties of sisal/oil palm hybrid fiber reinforced natural rubber composites. *Composites Science and Technology* 2004; 64:955-965.

30. P. Antich, Vazguez, I. Mondragon, C. Bernal. Mechanical behaviour of high impact polystyrene reinforced with short sisal fibres. *Composites Part A* 2006; 37:139-150.
31. K.C. Manikandan-Nair. S. Thomas, G. Groeninckx. Thermal and dynamic mechanical analysis of polystyrene composites reinforced with short sisal fibre. *Composites Science and Technology* 2001; 61:2519-2529.
32. S.T. Georgopoulos, P.A. Tarantili, E. Avgerinious, A.G. Andreopoloulos, E.G. Koukios. Thermoplastic polymers reinforced with fibrous agricultural residues. *Polymer Degradation and Stability* 2008; 90:303-312.
33. S.V. Joshi, L.T. Drazl, A.K. Mohanty, S. Arora. Are natural fiber composites environmentally superior to glass fiber reinforced composites? *Composites Part A* 2004; 35:371-376.
34. A.S. Singha, V.K. Thakur. Mechanical properties of natural fibre reinforced polymer composites. *Bulletin of Materials Science* 2008; 31(5):791-799.
35. M. Pracella, D. Chionna, I. Anguillesi, Z. Kulinski, E. Piorkowska. Functionalization, compatibilization and properties of polypropylene composites with hemp fibres. *Composites Science and Technology* 2006; 66:2218-2230.
36. C. Albano, J. Reyes, M. Ichazo, J. Gonzalez, M. Brito, D. Moronta. Analysis of the mechanical, thermal and morphological behaviour of polypropylene compounds with sisal fibre and wood flour, irradiated with gamma rays. *Polymer Degradation and Stability* 2002; 76:191-203.
37. C. Albano, A. Karam, D. Domínguez, Y. Sánchez, J. González, O. Aguirre, L. Cataño. Thermal, mechanical, morphological, thermogravimetric, rheological behaviour of HDPE/seaweed residues composites. *Composite Structures* 2005; 71:282-288.
38. X. Colom, F. Carrasco, P. Pages, J. Cañavate. Effects of different treatments on the interface of HDPE/lignocellulosic fibre composites. *Composites Science and Technology* 2003; 63:161-169.
39. W. Qui, T. Endo, T. Hirotsu. Structure and properties of composites of highly crystalline cellulose with polypropylene: effects of polypropylene molecular weight. *European Polymer Journal* 2006; 42:1059-1068.
40. J. George, S.S. Bhagawan, S. Thomas. Effects of environment on the properties of low-density polyethylene composites reinforced with pineapple leaf fibre. *Composites Science and Technology* 1998; 58:1471-1485.

41. P.V. Joseph, K. Joseph, S. Thomas, C.K.S. Pillai, V.S. Prasad, G. Groeninckx, M. Sarkissova. The thermal and crystallization studies of short sisal fibre reinforced polypropylene composites. *Composites Part A* 2005; 34:253-266.
42. J.R. Barone. Polyethylene/keratin fiber composites with varying polyethylene crystallinity. *Composites Part A* 2005; 36:1518-1524.
43. S. Mohanty, S.K. Verma, S.K. Nayak. Dynamic mechanical and thermal properties of MAPE treated jute/HDPE composites. *Composites Science and Technology* 2006; 66:538-547.
44. P.J. Herrera-Franco, A. Valadez-González. A study of the mechanical properties of short natural fiber reinforced composites. *Composites Part B* 2005; 36:597-608.
45. F.G. Torres, M.L. Cubillas. Study of the interfacial properties of natural fibre reinforced polyethylene. *Polymer Testing* 2005; 24:694-698.
46. X. Yaun, K. Jayaraman, D. Bhattacharrya. Effects of plasma treatment in enhancing the performance of wood fibre-polypropylene composites. *Composites Part A* 2004; 35:1363-1374.
47. F. Mengeloglu, A. Kabakci. Determination of thermal properties and morphology of eucalyptus wood residues filled high density polyethylene composites. *International Journal of Materials Science* 2008; 9:107-119.
48. M. Bengston, P. Gatenholm, K. Oksman. The effect of crosslinking on the properties of polyethylene/wood flour composites. *Composites Science and Technology* 2005; 65:1468-1479.
49. Y. Li, C. Hu, Y. Yu. Interfacial studies of sisal fiber reinforced high density polyethylene composites. *Composites Part A* 2008; 39:570-578.
50. K. Joseph, S. Thomas, C. Pavithran. Effect of ageing on physical properties of sisal fibre-reinforced polyethylene composites. *Composites Science and Technology* 1995; 53:99-110.
51. M. Kaci, H. Djidjelli, A. Boukerrou, L. Zaidi. Effect of wood filler treatment and EBAGMA compatibilizer on morphology and mechanical properties of low density polyethylene/oil husk flour composites. *eXPRESS Polymer Letters* 2007; 7(1):467-473.
52. K. Oksman, H. Lindberg. Influence of thermoplastic elastomers on adhesion in polyethylene-wood flour composites. *Journal of Applied Polymer Science* 1998; 68:1845-1855.
53. C.S.R. Freire, A.J.D. Silvestre, C.P. Neto, A. Gandini, L. Martin, I. Mondragon. *Composites Science and Technology* 2008; 68:3358-3364.

53. N.E. Marcovic, M.A. Villar. Thermal and mechanical characterization of linear low-density polyethylene/wood flour composites. *Journal of Applied Polymer Science* 2003; 90:2775-2784.
54. C-F. Kuan, H-C. Kuan, C-C.M. Ma, C-M. Huang. Mechanical, thermal and morphological properties of water-crosslinked wood flour reinforced linear low-density polyethylene composites. *Composites Part A* 2006; 37:1696-1707.
55. J-P. Kim, T-H, Yoon, S-P. Mun, Rhee, J-S. Lee. Wood-polyethylene composites using ethylene-vinyl alcohol copolymer as adhesion promoter. *Bioresource Technology* 1995; 53:99-110.
56. S.M.B. Nachtigall, G.S. Cerveira, S.M.L. Rosa. New polymeric-coupling agent for polypropylene/wood-flour composites. *Polymer Testing* 2007; 26:619-628.
57. P. Nygård, B.S. Tanem, T. Karlsen, P. Branchet, B. Leinsvang. Extrusion-based wood fibre-PP composites: wood powder and pelletized wood fibres – a comparative study. *Composites Science and Technology* 2008; 68:3418-3424.
58. X. Yuan, K. Jayaraman, D. Bhattacharyya. Effects of plasma treatment in enhancing the performance of woodfibre-polypropylene composites. *Composites Part A* 2004; 35:1363-1374.
59. S. Mohanty, S.K. Nayak. Dynamic and steady state viscoelastic behavior and morphology of MAPP treated PP/sisal composites. *Materials Science and Engineering A* 2007; 443:202-208.
60. K.L. Fung, R.K.Y. Li, S.C. Tjong. Interface modification on the properties of sisal fiber-reinforced polypropylene composites. *Journal of Applied Polymer Science* 2002; 85:165-176.
61. M. Pracella, D. Chionna, I. Anquillesi, Z. Kulinski, E. Piorkowska. Functionalization, compatibilization and properties of polypropylene composites with hemp fibres. *Composites Science and Technology* 2006; 66:2218-2230.
62. K.L. Pickering, G.W. Beckermann, S.N. Alam, N.J. Foreman. Optimising industrial hemp for composites. *Composites Part A* 2007; 38 (2):461-468.
63. J.Z. Lu, Q. Wu, I.I. Negulescu. Wood-fibre/high-density polyethylene composites: Coupling agent performance. *Journal of Applied Polymer Science* 2005; 96:93-102.
64. G. Sarkhel, A. Choudhury. Dynamic mechanical and thermal properties of PE-EPDM based jute fibre composites. *Journal of Applied Polymer Science* 2008; 108:3442-3453.

65. A. Viksne, L. Rence, M. Kalsnins, A.K. Bledzki. The effect of paraffin on fiber dispersion and mechanical properties of polyolefin-sawdust composites. *Journal of Applied Polymer Science* 2004; 93:2385-2393.
66. G-H. Doh, S-Y. Lee, I-A. Kang, Y-T. Kong. Thermal behavior of liquefied wood polymer composites. *Composite Structures* 2005; 68:103-108.
67. D. Pasquini, E. de M. Teixeira, A.A. da S. Curvedly, M. N. Belgacem, A. Dufresne. Surface esterification of cellulose fibres: processing and characterization of low-density polyethylene/cellulose fibres composites. *Composites Science and Technology* 2008; 68:193-201.
68. D. Harper, M. Wolcott. Interaction between coupling agent and lubricants in wood-polypropylene composites. *Composites Part A* 2004; 35:385-394.
69. A. Mahfuz, A. Adnan, V.K. Rangari, S. Jeelani, B.Z. Jang. Carbon nanoparticles/whiskers reinforced composites and their tensile response. *Composites Part A* 2004; 35:519-527.
70. S-M. Lai, F-C. Yeh, Y. Wang, H-C. Chan, H-F. Shen. Comparative study of maleated polyolefins as compatibilizers for polyethylene/wood flour composites. *Journal of Applied Polymer Science* 2003; 87:487-496.
71. H. Liu, Q. Wu, G. Han, F. Yao, Y. Kojima, S. Suzuki. Compatibilizing and toughening of bamboo flour-filled HDPE composites: Mechanical properties and morphologies. *Composites Part A* 2008; 39:1891-1900.
72. M.N. Ichazo, C. Albano, J. González. Behaviour of polyolefin blends with acetylated sisal fibres. *Polymer International* 2000; 49:1409-1416.
73. P.W. Balasuriya, L. Ye, Y-W. Mai. Mechanical properties of wood flakes-polyethylene composites. Part I: Effects of processing methods and matrix melt flow behaviour. *Composites Part A* 2001; 32:619-629.
74. Md. R. Rahman, Md. M. Haque, Md. N. Islam, M. Hassan. Mechanical properties of polypropylene composites reinforced with chemically treated abaca. *Composites Part A* 2009; 40(4):511-517.

Chapter 3

Materials and methods

3.1 Materials

3.1.1 Wax

Oxidized Fischer-Tropsch paraffin wax (OxWax) was used in this study. OxWax is an oxidized straight-hydrocarbon chain paraffin wax, average molar mass of 660 g mol^{-1} , with density of 0.95 g cm^{-3} (solid) and 0.82 g cm^{-3} (liquid) at $25 \text{ }^{\circ}\text{C}$ and $110 \text{ }^{\circ}\text{C}$ respectively, and has a melting point of $96 \text{ }^{\circ}\text{C}$. It has a thermal decomposition temperature of about $250 \text{ }^{\circ}\text{C}$, C/O ratio 18.8/1, and a flash point of approximately $185 \text{ }^{\circ}\text{C}$. It was supplied by Sasol Wax, Sasolburg, South Africa. The hard Fischer-Tropsch paraffin wax ($T_m = 90 \text{ }^{\circ}\text{C}$, $\rho = 0.94 \text{ g cm}^{-3}$, average $M_w = 785 \text{ g mol}^{-1}$) was also obtained from Sasol wax in South Africa.

3.1.2 Low-density polyethylene (LDPE)

LDPE was supplied in pellet form by Sasol Polymers, Johannesburg, South Africa. It has an MFI of 7.0 g/10min (ASTM D-1238), a melting point of $106 \text{ }^{\circ}\text{C}$, an average molar mass (MW) of 96000 g mol^{-1} , and a density of 0.918 g cm^{-3} .

3.1.3 Maleic anhydride (MAH) and dibenzoyl-peroxide (DBP)

Maleic anhydride (MAH) was supplied in flakes by Saarchem and dibenzoyl-peroxide (DBP) by Labchem in South Africa.

3.1.4 Sisal fibres

Sisal (*Agave sisalana*) fibre was obtained from the National Sisal Marketing Committee in Pietermaritzburg.

3.2 Methods

3.2.1 Preparation of maleic anhydride grafted Fischer-Tropsch wax (MA-g-wax)

A mixture of 85 wt % of wax, 10 wt% of MAH and 5 wt% of DBP was put into a round bottom flask with water-cooled temperature on top. The flask was immersed into an oil bath at 140 °C for 10 min and the reaction mixture was kept under a blanket of flowing nitrogen. After cooling the product was ground, immersed into boiling water, stirred for 10 min and filtered [1]. Unmodified and grafted wax was examined with Fourier-Transform infrared spectroscopy (FTIR; Fig. 3.1). For the maleated Fischer-Tropsch wax, the wavelengths of interest were 1704 cm^{-1} (characteristic of carbonyl from carboxylic dimmer acids) and 1745 cm^{-1} (characteristic of five-membered cyclic anhydride carbonyls) [2].

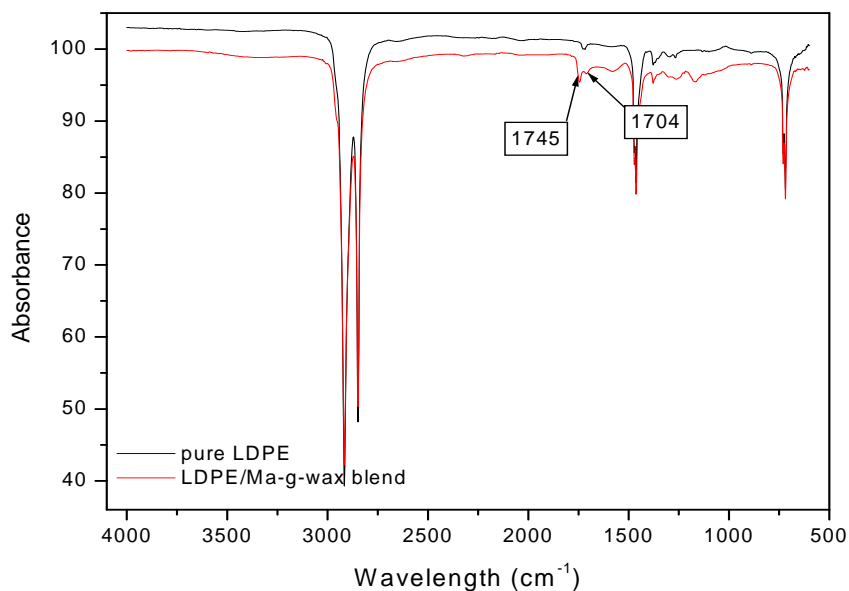


Figure 3.1 FTIR spectra for an unmodified Fischer-Tropsch wax (top) and the same wax grafted with 5 wt% MA (bottom).

3.2.2 Preparation of sisal fibres

The fibres were cut into ~ 9.0 mm using a pair of scissors. The fibres were soaked, and washed in petroleum ether for 6 hours to remove fatty impurities. To ensure easy blending of the fibres and the LDPE matrix, the fibres were washed thoroughly with warm distilled water

to remove petroleum ether traces [2]. Lastly, the fibres were allowed to air dry at room temperature for at least 4 days and then put in an oven at a temperature of 60 °C for 24 hours.

3.2.3 Preparation of the blends and composites

The blends and composites were prepared by weighing according to the desired ratios (Table 3.1) to make up a total mass of 36.7 g, the mass required to thoroughly mix the different components. The samples were initially mixed in a Brabender Plastograph at 160 °C at a screw speed of 15 rpm for 25 minutes. The samples were then melt pressed at 160 °C for 10 minutes at a pressure of 50 bar into 1 mm thick sheets.

Table 3.1 Sample compositions used in this study

LDPE/MA-g-wax blends (w/w)	LDPE/OxWax blends (w/w)	LDPE/sisal/MA-g-wax composites (w/w)	LDPE/sisal/OxWax composites (w/w)	LDPE/sisal composites (w/w)
100/0/0	100/0/0	100/0/0	100/0/0	100/0/0
95/5	95/5	85/10/5	85/20/5	90/10
90/10	90/10	80/10/10	80/10/10	80/20
-	-	75/20/5	75/20/5	70/30
-	-	70/20/10	70/20/10	-
-	-	65/30/5	65/30/5	-
-	-	60/30/10	60/30/10	-

3.2.4 Differential scanning calorimetry (DSC)

Differential scanning calorimetry is a technique used to study thermal transitions of a polymer. Thermal transitions are the changes that take place in a polymer when it is heated or cooled at a controlled rate. The melting and crystallization of a crystalline polymer, as well as its glass transition are typical examples of thermal transitions. In DSC systems, two pans containing respectively the polymer sample (1-10 mg) and an inert solid are individually heated or cooled. The DSC measures the difference in electrical power (ΔQ) supplied to the two pans as function of time or temperature.

The DSC used is a Perkin Elmer Pyris-1 DSC from Waltham, Massachusetts, U.S.A. Analyses were performed under flowing nitrogen (20 mL min^{-1}). The instrument was computer controlled and calculations were done using Pyris software. The instrument was calibrated using the onset temperatures of melting of indium and zinc standards, as well as the melting enthalpy of indium. 5-10 mg samples were sealed in aluminium pans, heated from 0 to $160 \text{ }^{\circ}\text{C}$ at a heating rate of $10 \text{ }^{\circ}\text{C min}^{-1}$, and cooled at the same rate to $0 \text{ }^{\circ}\text{C}$. For the second scan, the samples were heated and cooled under the same conditions. The onset and peak temperatures of melting and crystallization, as well as the melting and crystallization enthalpies were determined from the second scan.

3.2.5 Thermogravimetric analysis (TGA)

TGA is an important analytical method in understanding the structure-property relationships and thermal stability of composites materials. It also offers a more precise control of heating condition, such as variable temperature range and accurate heating rate, and needs only a small quantity of sample for analysis. It is mainly used to determine the moisture content and volatile components resulting from degradation [4-5]. The most widely used TGA method is based on a continuous measurement of mass on a sensitive balance, called a thermobalance, as the sample temperature is increased in air or in an inert atmosphere. This is referred to as nonisothermal TGA. Data are recorded as a TGA curve of mass or mass % as function of temperature or time. Mass loss may arise from evaporation of residual moisture or solvent, but at higher temperatures it results from polymer decomposition. Besides providing information on thermal stability, TGA may be used to characterize polymers through loss of a known entity, such as HCl from poly(vinyl chloride). TGA is also useful for determining volatilities of plasticizers and other additives.

The TGA used was a Perkin Elmer TGA7 from Waltham, Massachusetts, U.S.A. Analyses were performed under flowing nitrogen at a flow rate of 20 mL min^{-1} . The instrument was computer controlled and calculations were done using Pyris software. Samples (5-10 mg) were heated from 25 to $600 \text{ }^{\circ}\text{C}$ at $20 \text{ }^{\circ}\text{C min}^{-1}$.

3.2.6 Dynamic mechanical analysis (DMA)

Dynamic mechanical analysis (DMA) has been a well established method in thermal analysis for many years. A DMA measurement consists of the observation of time-dependent

deformation behaviour $x(t)$ of a sample under periodic, mostly sinusoidal deformation force with very small amplitudes, $F(t)$. Thus, this makes it possible to calculate, for instance, Young's modulus E' (storage modulus) and E'' (loss modulus) and the mechanical loss factor $\tan \delta$ (damping). This sensitive technique (DMA) characterizes the mechanical responses of materials by monitoring property changes with respect to temperature and/or frequency of oscillation. The technique separates the dynamic response of materials into two distinct parts (i) an elastic part (E') (ii) and a viscous part or damping component (E''). The elastic process describes the energy stored in the system, whereas the viscous component describes the energy dissipated during the process. For natural fibre/thermoplastic composites, both phases exhibit viscoelastic behaviour. It is interesting to note that DMA provides rapid assessment on the viscoelastic properties of these materials, despite the controversy following the discussion of the relaxation mechanism in polyethylene. DMA measurements conducted over a wide range of temperatures helps to study the viscoelastic behaviour of molten polymer systems, particularly the glass transition region in the reinforced composites. Contrary to the established instruments for quasi-static determination of the elastic parameters from stress strain testing, DMA only requires samples with a small mass or size [6-8].

The dynamic mechanical properties of the blends and composites were investigated using a Perkin Elmer Diamond DMA from Waltham, Massachusetts, U.S.A. The settings for the analyses were as follows:

Frequency	1 Hz
Amplitude	20 μm
Temperature range	-140 to 100 $^{\circ}\text{C}$
Heating rate	5 $^{\circ}\text{C min}^{-1}$
Preload force	0.02 N
Sample length	20 mm
Sample width	12.0 – 12.5 mm
Sample thickness	1.0 – 1.3 mm

3.2.7 Tensile testing

A tensile test, also known as a tension test, is a measure of material reaction to applied forces. For most materials, the initial relationship between the applied force, or load, and the elongation the specimen exhibits, is linear. In this linear region, the line obeys the relationship

defined as "Hooke's Law" where the ratio of stress to strain is a constant, or $\sigma/\epsilon = E$. E is the slope of the line in this region where stress (σ) is proportional to strain (ϵ) and is called the modulus of elasticity or Young's modulus. This is a measure of the stiffness of the material, but it only applies in the initial linear region of the curve. Within this linear region, the material will return to its exact same condition if the load is removed. At the point that the curve is no longer linear and deviates from the straight-line relationship, Hooke's Law no longer applies and some permanent deformation occurs in the specimen. This point is called the elastic, or proportional, limit, or the yield point. From this point on in the tensile test, the material reacts plastically to any further increase in load or stress. It will not return to its original, unstressed condition if the load were removed.

A Hounsfield H5KS universal testing machine from Redhill, United Kingdom was used for the tensile analysis of the samples. The dumbbell samples were stretched at a speed of 50 mm min⁻¹ under a cell load of 2500 N. The gauge length was 24 mm, the thickness was 1.0 ± 0.1 mm and the width was 4.8 mm. The final mechanical properties were evaluated from 5 different measurements.

3.2.8 Scanning electron microscopy (SEM)

During SEM analysis, electrons from a filament in an electron gun are beamed at the specimen in a vacuum chamber. The beam forms a line that continuously sweeps across the specimen surface at high speed. This beam irradiates the specimen which in turn produces a signal in the form of either x-ray fluorescence, secondary or backscattered electrons. The scan rate for the electron beam can be increased so that a virtual 3-D image of the specimen can be viewed. The image can also be captured by standard photography. SEM images have great depth of field yielding a characteristic three-dimensional appearance useful for understanding the surface structure of a sample e.g. the interfacial adhesion in composites.

SEM analyses were carried out in a JEOL WINSEM-6400 scanning electron microscope from Tokyo, Japan. The probe size was 114.98 nm, the probe current 0.02 nA, the noise reduction 64 Fr and the AC voltage 5.0 keV. The surfaces of the samples were coated with gold.

3.4 References

1. H. Krump, P. Alexy, A.S. Luyt. Preparation of a maleated Fischer-Tropsch paraffin wax and FTIR analysis of grafted maleic anhydride. *Polymer Testing* 2005; 24:129-135.
2. I. Novák, I. Krupa, A.S. Luyt. Modification of the polarity and adhesive properties of polyolefins through blending with maleic anhydride grafted Fischer-Tropsch paraffin wax. *Journal of Applied Polymer Science* 2006; 100:3069-3074.
3. M.A. Mokoena, V. Djoković, A.S. Luyt. Composites of linear low density polyethylene and short sisal fibres: the effects of peroxide treatment. *Journal of Materials Science* 2004; 39:3403-3412.
4. K.C. Manikandan-Nair, S. Thomas, G. Groeninckx. Thermal and mechanical analysis of polystyrene composites reinforced with short sisal fibres. *Composites Science and Technology* 2001; 61:2519-2529.
5. J. George, S.S. Bhagawan, S. Thomas. Thermogravimetric and dynamic mechanical thermal analysis of pineapple fibre reinforced polyethylene composites. *Journal of Thermal Analysis* 1996; 47:1121-1140.
6. B. Wielage, Th. Lampke, H. Utschick, F. Soergel. Processing of natural-fibre reinforced polymers and resulting dynamic-mechanical properties. *Journal of Materials Processing Technology* 2003; 139:140-146.
7. S. Mohanty, S.K. Verma, S. K. Nayak. Dynamic mechanical and thermal properties of MAPE treated jute/HDPE composites. *Composites Science and Technology* 2006; 66:538-547.
8. T. Mehdi, H.F. Robert, C.H. John, F. Colin. Influence of natural fibers on the phase transitions in high-density polyethylene composites using dynamic mechanical analysis. *The Seventh International Conference on Woodfiber-Plastic Composites*. Wisconsin, USA (19-20 May 2003).

Chapter 4

Results and discussion

4.1 Scanning electron microscopy (SEM)

The morphology of the fractured surfaces of untreated and treated composites at 30% sisal content studied by SEM analysis is illustrated in Figures 4.1 to 4.3. For each material, two magnifications were used to display both the fibre dispersion and the interfacial adhesion. The untreated composite shows a large number of holes (Figure 4.1a, A) in the LDPE matrix resulting from fibre pullout. There are also distinct gaps between the fibres and the matrix. It can be further seen that there is agglomeration of fibres in the LDPE matrix (Figure 4.1a, B), and the fibres are free of any matrix adhering to them (Figure 4.1b, C). Sarkhel and Choudhury [1] investigated PE-EPDM blends and jute reinforced PE-EPDM composites treated with different concentrations of maleic anhydride grafted polyethylene. For the untreated composites, the fibres appeared to be free from the polymer matrix, and a large number of holes or voids resulting from extensive fibre pullout were observed. These features were related to poor interfacial adhesion and inadequate wetting of the untreated fibre within the non-polar PE-EPDM matrix, which is due to large differences in surface energies between the fibre and the matrix. This is in agreement with observations by other authors [2-3].

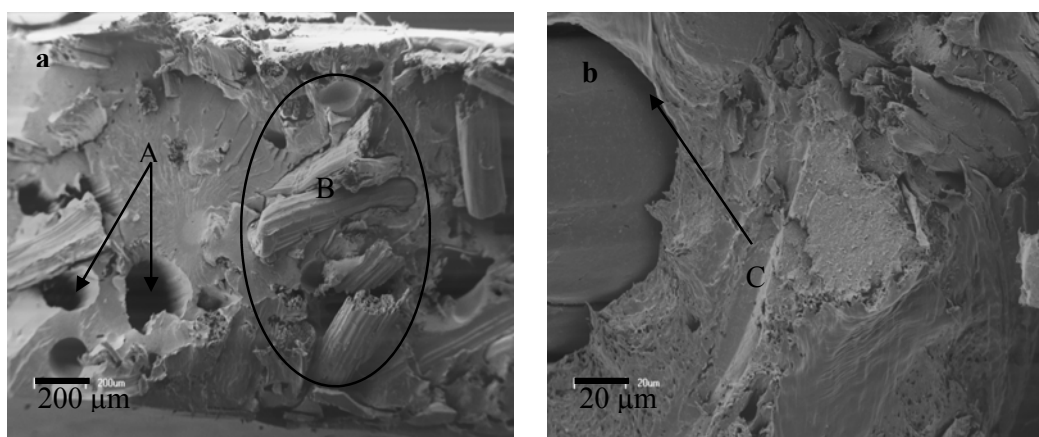


Figure 4.1 SEM micrographs for uncompatibilized 70/30 w/w LDPE/sisal composites at 100x and 1000x magnifications

Figure 4.2 shows the morphology of the LDPE/sisal/OxWax composites. In the presence OxWax there are no signs of fibre agglomeration, and fewer fibre pullouts from the matrix compared to the LDPE/sisal composites are observed. The sisal fibres appear to be completely covered by OxWax (Figure 4.2a). Phase separation between the LDPE matrix and OxWax is visible (Figure 4.2b). This separate crystallization behaviour is a result of the low molecular weight as well as lower viscosity of OxWax. It is possible to observe holes due to fibre pullouts from the matrix, with some fibres adhering to the matrix (Figure 4.3c). There are no gaps between the LDPE matrix and the fibre (Figures 4.3a and 4.3c), indicating better adhesion. However, fairly good wax distribution within LDPE matrix is observed (Figure 4.3b), if we assume the white phase to be the wax. However, this may be a risky assumption in view of the fact that differences in topology will also give different coloured regions.

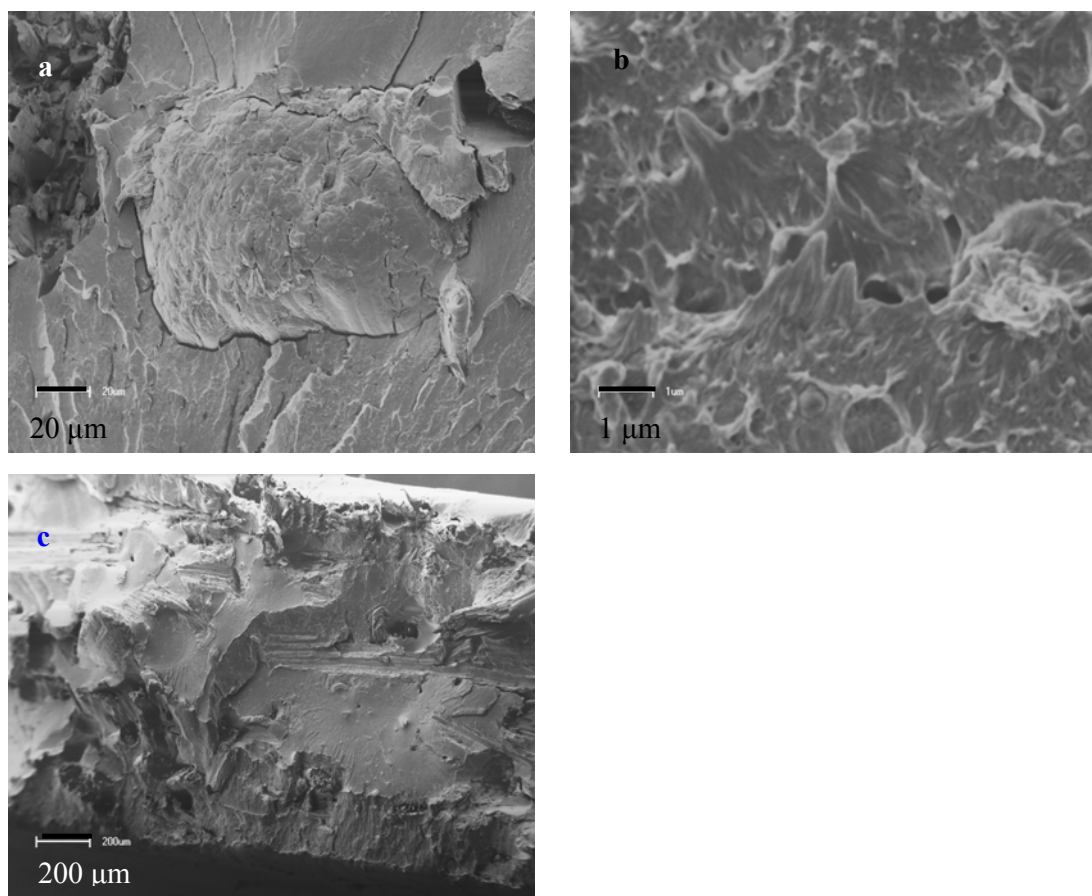


Figure 4.2 SEM micrographs for compatibilized 65/30/5 w/w LDPE/sisal/OxWax composites at 1000x, 20000x and 100x magnifications.

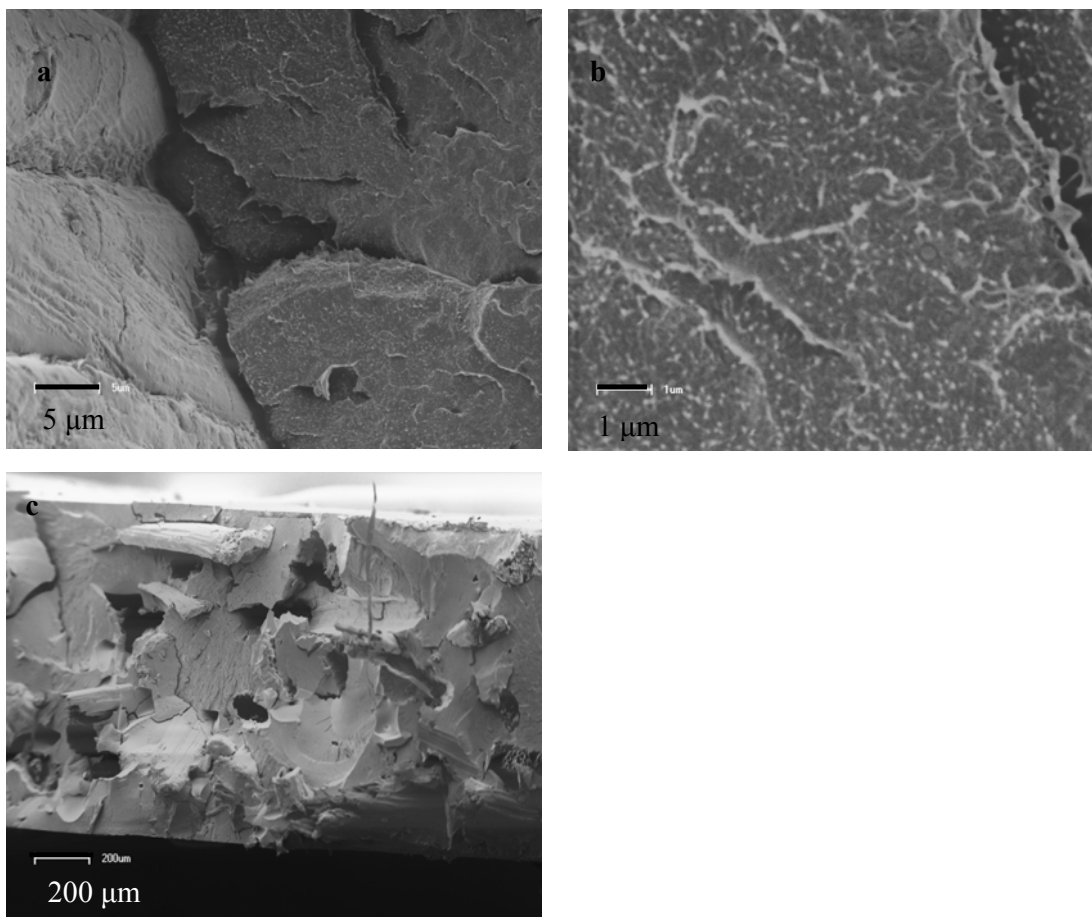


Figure 4.3 SEM micrographs for compatibilized 65/30/5 w/w LDPE/sisal/MA-g-wax composites at 4800x, 20000x and 1000x magnifications.

4.2 Differential scanning calorimetry (DSC)

All the DSC heating curves were taken from the second heating scan to eliminate the effect of the thermal history. The heating curves of untreated LDPE/sisal composites, blends and treated composites are shown in Figures 4.4 to 4.8 while the values of the melting peak temperatures, as well as the experimental and calculated enthalpies are summarized in Table 4.1. The measured melting enthalpy (ΔH_m^{obs}) values were compared with the calculated values (ΔH_m^{calc}) (Table 4.1). The ΔH_m^{calc} values were determined from the melting enthalpies of pure LDPE and pure wax, and the weight fractions of LDPE and wax in the respective blends according to the additive rule in Equation 4.1. Here we assume sisal fibre to have no effect on the LDPE and wax crystallization behaviour.

$$\Delta H_m^{calc} = \Delta H_{m,PE} w_{PE} + \Delta H_{m,w} w_w \quad (4.1)$$

where $\Delta H_{m,PE}$, $\Delta H_{m,w}$, ΔH_m^{add} are the specific enthalpies of melting of PE, wax and blends, and w_{PE} , w_w are the weight fractions of PE and wax in the blends.

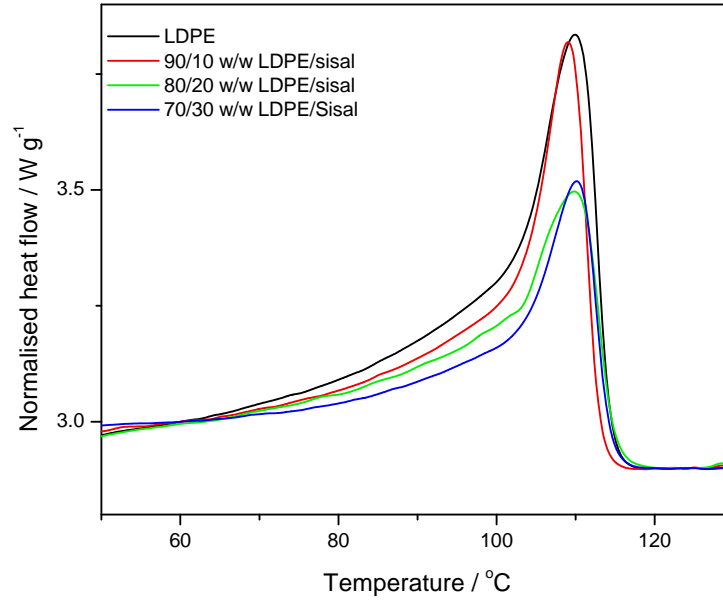


Figure 4.4 DSC heating curves of pure LDPE and LDPE/sisal composites

Figure 4.4 shows the DSC heating curves for pure LDPE and LDPE/sisal composites with different sisal contents. Only one endothermic peak was observed around the melting temperature of LDPE. Generally, there was no change in melting peak temperature with increasing fibre content (Table 4.1). The presence of sisal fibre also does not seem to influence the melting enthalpy of the composites, which can be seen from the observed and calculated melting enthalpy values, which are almost the same within experimental error. As expected, the measured enthalpy values decrease, because only LDPE melts, and there are decreasing amounts of LDPE in the samples with increasing sisal content. The fact that there are no changes in the melting temperature, and that the observed and calculated melting enthalpies are almost the same, is an indication that the fibre had very little influence on the crystallization mechanism of LDPE.

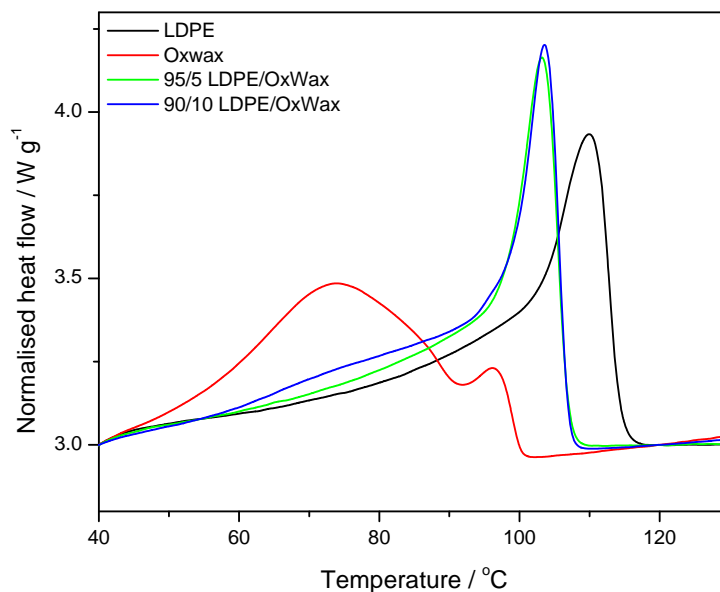


Figure 4.5 DSC heating curves of pure LDPE and LDPE/OxWax blends

Figures 4.5 and 4.6 show the DSC heating curves of the LDPE/OxWax and LDPE/MA-g-wax blends, respectively. The neat OxWax shows two well defined separate peaks at 73 and 96 °C, and the neat MA-g-wax shows peaks at 79 and 105 °C. Luyt and Krupa [4] reported that the multiple endothermic peaks of hard paraffin waxes were due to the melting of different molar mass fractions. Only one endothermic peak was seen for the 5% OxWax containing blend, indicating miscibility of LDPE and OxWax at this wax content (Figure 4.5). However, in the case of the 10% OxWax blend there was an additional peak around the wax melting temperature. This could be attributed to the partial immiscibility of OxWax and LDPE at higher wax contents. The presence of OxWax reduces the melting temperature of LDPE, with relatively no change as the OxWax content increases. This could be the result of the molten wax which acts as a plasticizer in the LDPE matrix. The introduction of OxWax in LDPE has no significant effect on the melting enthalpy of the blends. However, the higher OxWax content resulted in an increased enthalpy approaching that of pure LDPE (Table 4.1). The increased crystallinity of the sample caused by the wax crystals in the amorphous phase of the polymer, and the higher melting enthalpy of the wax, is the most probable reason for this observation. This is to be expected since the OxWax has a higher melting enthalpy than the pure LDPE. The presence of 5 and 10 wt% OxWax in LDPE does not seem to influence the melting enthalpy values, which can be noticed from the calculated and observed melting enthalpies that are similar within experimental error.

Table 4.1 DSC results for LDPE, LDPE/MA-g-wax and LDPE/OxWax blends, as well as LDPE/sisal, LDPE/sisal/MA-g-wax and LDPE/sisal/OxWax composites

Sample w/w	$T_{p,m} / ^\circ\text{C}$	$\Delta H_m^{obs} / \text{J g}^{-1}$	$\Delta H_m^{calc} / \text{J g}^{-1}$
LDPE			
100/0	110.3	53.6	-
LDPE/sisal			
90/10	109.4	49.0	48.2
80/20	110.0	43.7	42.9
70/30	110.0	38.5	37.5
LDPE/OxWax			
95/5	103.5	52.3	53.8
90/10	103.8	52.6	54.0
0/100	75.2 ^a 96.5 ^b	57.3	-
LDPE/MA-g-wax			
95/5	109.0	49.6	57.0
90/10	109.2	52.8	60.3
0/100	105.3 ^a 73.0 ^b	120.9	-
LDPE/sisal/OxWax			
85/10/5	104.5	50.4	48.4
80/10/10	104.4	49.0	48.6
75/20/5	104.0	41.1	43.1
70/20/10	104.5	32.9	43.2
65/30/5	104.9	25.9	37.7
60/30/10	105.0	24.8	37.9
LDPE/sisal/MA-g-wax			
85/10/5	109.0	55.5	51.6
80/10/10	109.0	45.9	55.0
75/20/5	109.9	43.4	46.2
70/20/10	109.4	39.3	49.6
65/30/5/	110.5	36.3	40.0
60/30/10	109.7	31.8	38.2

$T_{p,m}$, ΔH_m^{obs} and ΔH_m^{calc} are the melting peak temperature, observed melting enthalpy, calculated melting enthalpy

The melting behaviour of the LDPE/MA-g-wax blends is similar to that of pure LDPE (Figure 4.6), which suggests possible co-crystallization of PE and wax chains. Hlangothi *et al.* [5] reported on the influence of the wax content and different concentrations of the crosslinking agent on the properties of LLDPE/wax blends. It was found that the melting behaviour of all the un-crosslinked blends were similar to that of pure LLDPE. This was explained as indicating possible co-crystallization of PE and wax chains. MA-g-wax has a much higher enthalpy value compared to pure LDPE (Table 4.1). The observed melting enthalpy values of the blends are lower than the calculated values. This shows that the presence of MA-g-wax lowered the crystallinity of the blends. This is probably the result of the better interaction

between LDPE and MA-g-wax, which led to better miscibility between these two components, and as a consequence there were fewer wax crystals in the amorphous phase of the LDPE.

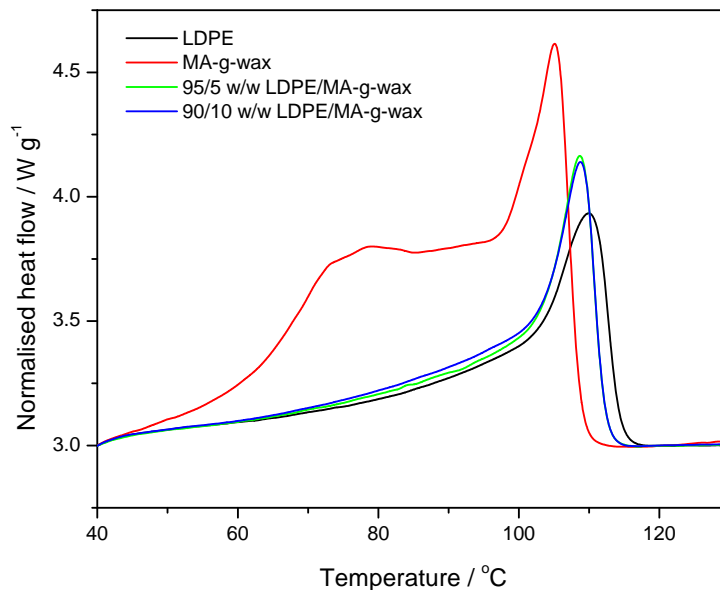


Figure 4.6 DSC heating curves of pure LDPE and LDPE/MA-g-wax blends

The DSC heating curves of LDPE/sisal/OxWax and LDPE/sisal/MA-g-wax composites are respectively shown in Figures 4.7 and 4.8. There is only one endothermic peak around the melting temperature of LDPE. The melting peak temperatures for the LDPE/sisal/OxWax composites are lower than that of pure LDPE (Figure 4.7 and Table 4.1). Similar to the blends, this is a consequence of the plasticization of the LDPE matrix by the wax. The observed and calculated melting enthalpy values are almost the same for the 10% fibre containing samples, while the differences between the observed and calculated values become bigger with increasing fibre content. This may be the result of the complete coverage of the fibres by OxWax at the lower fibre content, which led to the fibres having no influence on the LDPE crystallization behaviour. The increase in differences between the observed and calculated values may be the result of more wax crystals in the amorphous phase of the LDPE, which probably immobilized the polymer chains and gave rise to reduced crystallization. It can be seen in Figure 4.8 that the melting peak temperatures of the composites in the presence of MA-g-wax remained fairly constant with increasing sisal and MA-g-wax contents, within experimental error. Similar to the OxWax composite systems, the experimentally observed

melting enthalpies of the LDPE/sisal/MA-g-wax are lower than the calculated enthalpies for all the investigated wax contents, except for the 85/10/5 w/w LDPE/sisal/MA-g-wax sample. Similar to the blends, this may be the result of the better miscibility of MA-g-wax with the LDPE matrix.

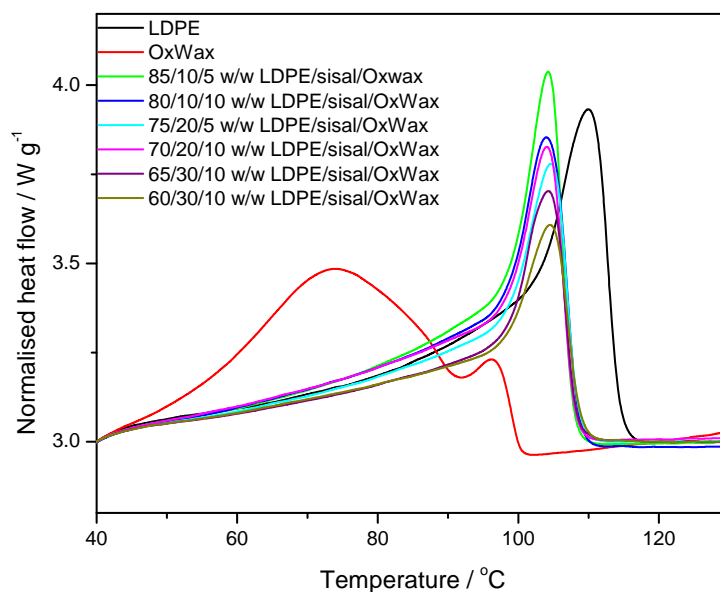


Figure 4.7 DSC heating curves of pure LDPE and LDPE/sisal/OxWax composites

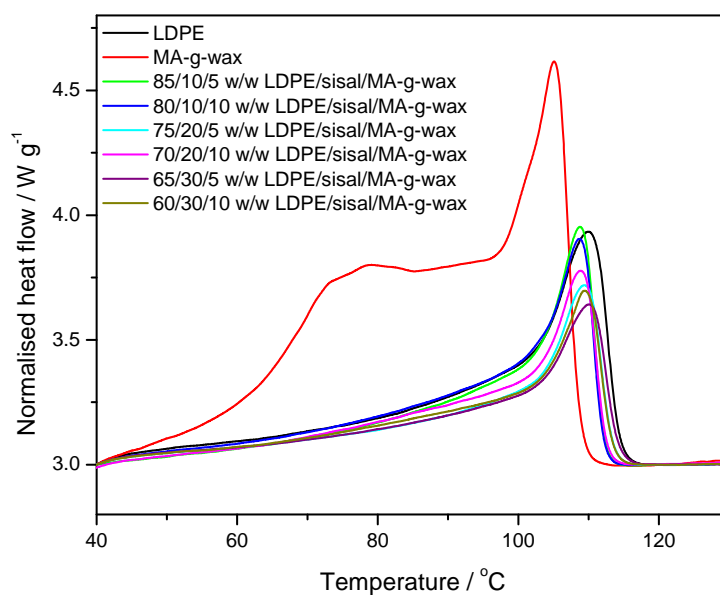


Figure 4.8 DSC heating curves of pure LDPE and LDPE/sisal/MA-g-wax composites

4.3. Thermogravimetric analysis (TGA)

The TGA curves of LDPE, sisal and OxWax, as well as an LDPE/OxWax blend and LDPE/sisal/OxWax composites are shown in Figure 4.9. LDPE has a higher thermal stability than both OxWax and sisal fibre. Both pure LDPE and OxWax degraded in one step. However, the sisal fibre shows multiple degradation steps. The step observed at 65 °C is due to the vaporization of moisture from the fibre (stage 1). The second step at about 365 °C is due to the thermal depolymerisation of hemicellulose and the cleavage of glycosidic linkage of cellulose (stage 2). The third step (at about 400 °C) may be due to the further break-down of the decomposition products of stage 2, leading to the formation of char through levoglucosan [6-7].

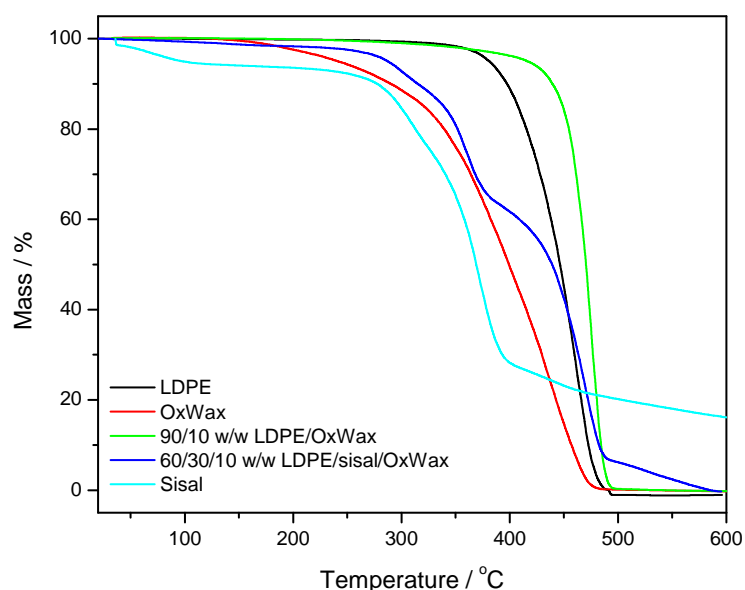


Figure 4.9 TGA curves of pure LDPE, OxWax, sisal, 90/10 LDPE/OxWax blend and 60/30/10 LDPE/sisal/OxWax composite

The LDPE/OxWax blend decomposed at a higher temperature than pure LDPE and the OxWax containing composite. The degradation mechanism of the LDPE/OxWax blends is not yet well understood. However, possible reasons for the increase in thermal stability of these blends may be that the wax crystals in the amorphous phase of the polymer are initially protected by the surrounding, thermally more stable polymer chains. The crystallites may then also immobilize free radical chain sections or volatile degradation products, which gives rise

to a significantly higher onset temperature of mass loss. Krupa *et al.* [8] used TGA to evaluate the thermal stability of LDPE/OxWax blends as phase change materials and found that the thermal stability of the blends decreased with an increase in OxWax content. They explained this behaviour as being a consequence of the lower thermal stability of OxWax. However, Djoković *et al.* [9] observed similar behaviour to that in the current study, whereby the presence of 5 and 10% OxWax in LDPE showed improved thermal stability of more than 50 °C. They attributed this behaviour to the co-crystallization of OxWax and LDPE.

In the case of the LDPE/sisal/OxWax composite four degradation steps are observed. The first decomposition step at 100 °C corresponds to the evaporation of moisture in the composites. The second step at 279 °C corresponds to the degradation of cellulose. The third step at 346 °C is a combination of the degradation of cellulose and OxWax. The fourth step at 400 °C is due to the degradation of the unsaturated and saturated carbon atoms of LDPE. At 500 °C, char formation is observed for LDPE/sisal/OxWax composites.

In Figure 4.10, the TGA curves of LDPE, sisal, MA-g-wax, an LDPE/MA-g-wax blend and an LDPE/sisal/MA-g-wax composite are depicted. The LDPE has a higher thermal stability than the MA-g-wax. The blend has a slightly higher thermal stability than the pure LDPE. This is probably a consequence of the co-crystallization of MA-g-wax and LDPE as seen by DSC [8], where the less thermally stable wax chains are protected in the thicker lamellae. The thermal stabilities of the composites are lower than that of pure LDPE as a consequence of the lower thermal stability of both wax and sisal fibre, and because the wax crystallized around the fibre. The fibre probably starts to degrade first and provides the free radicals that initiate the wax degradation, which further initiates the LDPE degradation. Similar to the OxWax composite system, the MA-g-wax composite system shows multiple degradation steps. In contrast to the OxWax composite system, the MA-g-wax composite system has a lower thermal stability than the neat MA-g-wax, which is more stable because of the presence of maleic anhydride units on the backbone of the wax.

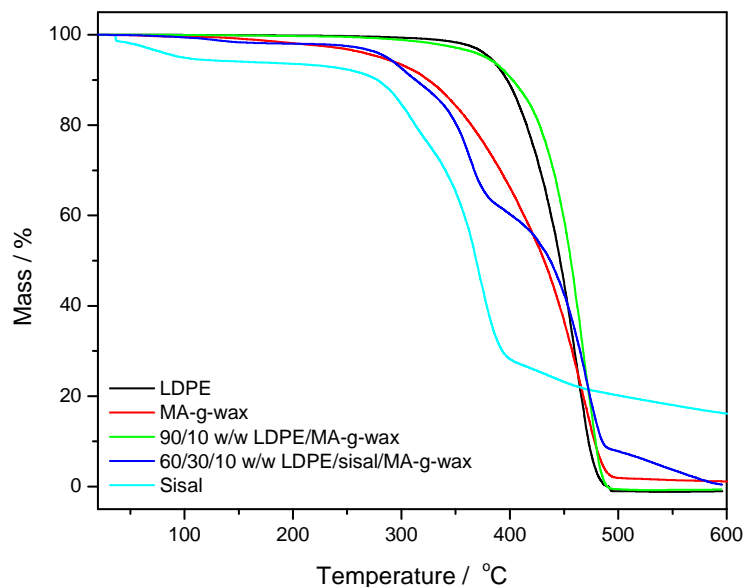


Figure 4.10 TGA curves of pure LDPE, MA-g-wax, sisal, 90/10 w/w LDPE/MA-g-wax blend and 60/30/10 w/w LDPE/sisal/MA-g-wax composite

4.4 Tensile properties

The stress at break, elongation at break and modulus of all the samples are summarized in Table 4.2 and shown in Figures 4.11 to 4.16. The effect of OxWax and MA-g-wax content on the stress at break is shown in Figures 4.11 and Figure 4.12, respectively. Samples prepared in the absence of wax show an increase in stress at break for 10 and 20% sisal, with the 20% containing sample showing a maximum (Figure 4.11). Vilaseca *et al.* [10] investigated the composite system of PP and abaca strands in the absence and presence of maleated polypropylene. They found that the tensile strength of the untreated composites increased remarkably with increasing abaca content. They associated this behaviour with the mechanical anchoring between the fibre and the matrix, and to the diffusion of the polymer into the fibre. This is in agreement with other authors [11-12] who reported similar phenomena. Possible reasons for the decline in stress at break at high fibre content are: (i) poor interfacial adhesion, which promotes microcrack formation at the interface as well as non-uniform stress transfer because of fibre agglomeration (fibre-fibre contact which results in fibre damage) within the LDPE matrix, and (ii) an increase in the number of voids in the composites that serve as local areas for crack initiation [13].

Table 4.2 Tensile testing data

Sample			
w/w	$\epsilon_b \pm s\epsilon_b$ / %	$\sigma_b \pm s\sigma_b$ / MPa	$E \pm sE$ / MPa
LDPE			
100/0	76 ± 6.5	7.6 ± 0.6	49.0 ± 19.8
LDPE/ sisal			
90/10	16.1 ± 1.6	9.2 ± 0.6	138 ± 16
80/20	12 ± 0.9	17.2 ± 1.6	406 ± 8
70/30	10.0 ± 1.9	11.0 ± 0.9	244 ± 48
LDPE/ OxWax			
95/5	21.4 ± 2.2	8.4 ± 0.2	120 ± 3
90/10	20.2 ± 0.7	9.0 ± 0.3	141 ± 9
LDPE/MA-g-wax			
95/5	63.9 ± 4.3	8.4 ± 0.5	77.0 ± 2.7
90/10	76.1 ± 10.1	8.3 ± 0.3	94.9 ± 5.0
LDPE/sisal/OxWax			
85/10/5	10.3 ± 1.8	7.3 ± 0.5	219 ± 6
80/10/10	11.2 ± 1.1	7.0 ± 0.3	206 ± 4
75/20/5	5.0 ± 0.6	10.9 ± 0.8	445 ± 7
70/20/10	5.5 ± 0.9	6.6 ± 0.8	413 ± 18
65/30/5	4.2 ± 0.7	10.9 ± 2.4	537 ± 31
60/30/10	3.2 ± 0.94	8.4 ± 0.8	465 ± 28
LDPE/sisal/MA-g-wax			
85/10/5	9.1 ± 0.8	6.9 ± 0.4	50 ± 23
80/10/10	4.6 ± 1.8	9.5 ± 0.9	269 ± 67
75/20/5	4.4 ± 1.8	9.2 ± 0.8	323 ± 63
70/20/10	5.8 ± 0.5	10.1 ± 0.5	440 ± 43
65/30/5/	3.6 ± 0.5	9.1 ± 0.8	454 ± 10
60/30/10	3.6 ± 0.4	11.1 ± 2.3	515 ± 84

σ_b is the stress at break and $s\sigma_b$ is the standard deviation, ϵ_b is the elongation at break and $s\epsilon_b$ is the standard deviation, E is Young's modulus and sE is the standard deviation

For both the 5 and 10 % OxWax containing samples there is an observable decrease in tensile strength with increasing sisal fibre content up to about 15% fibre, with an increase at higher sisal fibre contents. The initial decrease in tensile strength is probably because at lower fibre contents the fibre is completely covered by wax, and because there seems to be a weaker interaction between LDPE and the wax. At higher fibre contents there is not enough wax to completely cover the fibres, and there may be better interaction between the LDPE and the fibres because of mechanical interlocking. This may lead to better stress transfer and

increasing tensile strength. Similar observations were reported by Kim *et al.* [14], where the mechanical properties of PP/cotton fibre composites were compared with those of PP/wood fibre composites. Figure 4.12 shows the stress at break for the MA-g-wax containing samples. Generally the tensile strength increases with an increase in sisal content. This could be a consequence of MA-g-wax interacting more strongly with LDPE and, because the wax was concentrated around the fibre, there is a stronger interaction between LDPE and the filler.

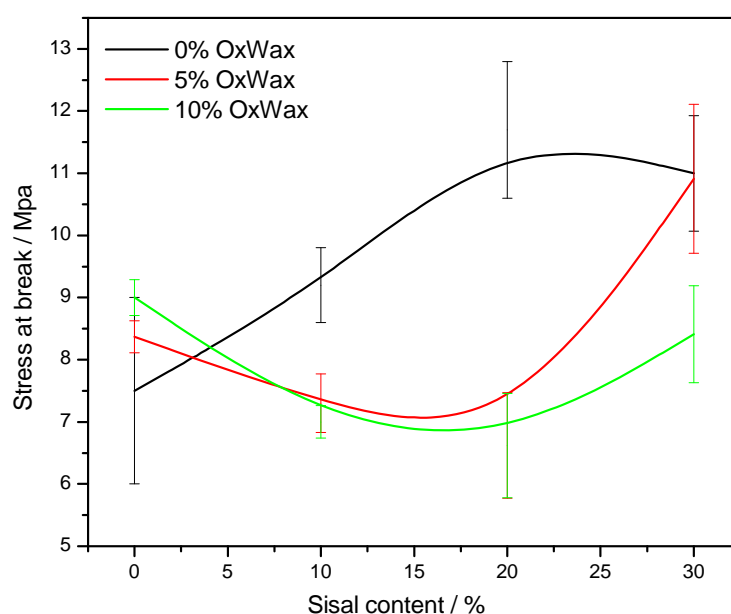


Figure 4. 11 Stress at break as function of sisal content for the LDPE/sisal/OxWax composites

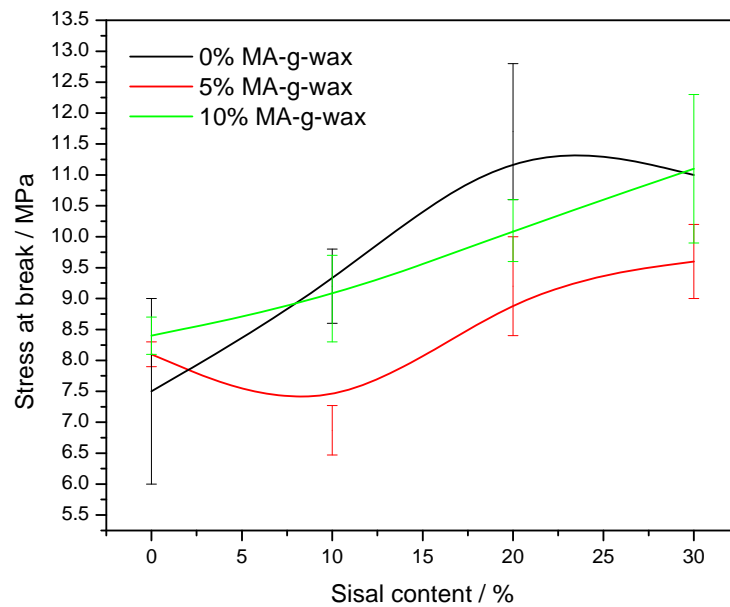


Figure 4.12 Stress at break as function of sisal content for the LDPE/sisal/MA-g-wax composites

The effect of OxWax and MA-g-wax content on the elongation at break are shown in Figures 4.13 and 4.14. In Figure 4.13, it can be seen that the elongation at break decreases with increasing sisal content. This indicates that the presence of fibre in the matrix reduces the ability of the sample to deform. Figure 4.14 shows a general decrease in elongation at break with an increase in sisal fibre content. This is normal for polymers containing rigid fillers, because the fillers act as defect centres that give rise to reduced stress transfer. The presence of OxWax considerably reduced the elongation at break, while the presence of MA-g-wax only slightly reduced the elongation at break. In the case of MA-g-wax, this could be associated with a better interaction between the polymer and the MA-g-wax and therefore better stress transfer. The OxWax behaved differently due to the crystallization of the wax in the amorphous phase of the LDPE, and which formed defect centres in the polymer matrix.

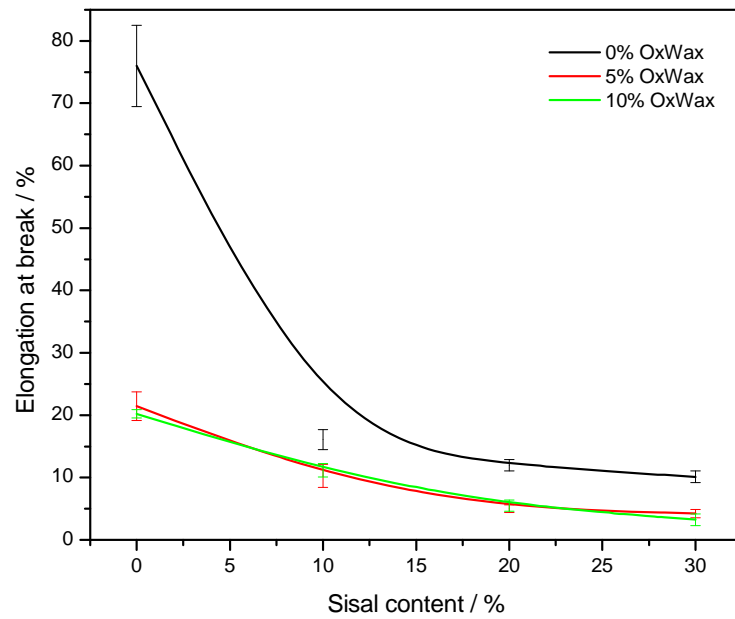


Figure 4.13 Elongation at break as a function of sisal content for the LDPE/sisal/ OxWax composites

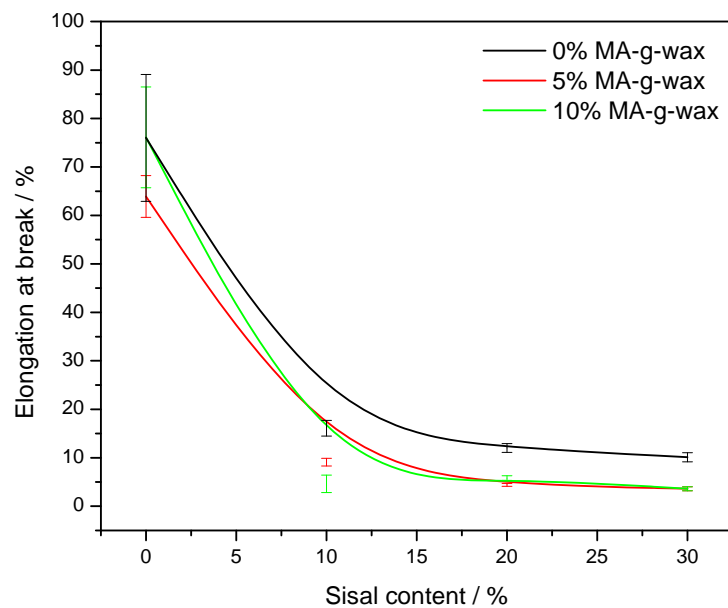


Figure 4.14 Elongation at break as a function of sisal content for the LDPE/sisal/ MA-g-wax composites

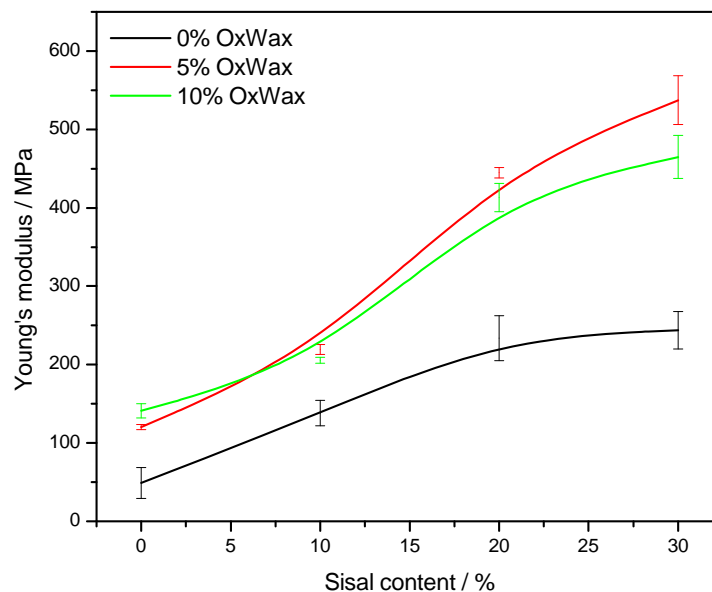


Figure 4.15 Young's modulus as function of sisal content for the LDPE/sisal/OxWax composites

Figures 4.15 and 4.16 show the effect of fibre and wax contents on the Young's modulus values of the samples. For all the composites there was a general increase in Young's modulus with increasing sisal content. An increase in OxWax content does not show much influence on the modulus values (Figure 4.15), but these values are significantly higher than those of the composites prepared in the absence of wax, and this difference becomes bigger with increasing sisal content. This can be attributed to the higher degree of crystallinity of the OxWax, as can be seen from the DSC results (Table 4.1). The higher modulus values in the 5% OxWax containing sample is the result of partial miscibility between LDPE and OxWax, as observed from SEM and supported by the DSC results, while the behaviour of the 10% OxWax containing sample is the result of higher immiscibility leading to wax forming crystals in the amorphous phase of the polymer. The modulus values increased with increasing sisal content, because the wax completely covered the sisal fibre at low fibre contents, but only partially at higher fibre contents. Because the LDPE seems to interact more strongly with the fibre than with the wax, the uncovered fibre probably had a bigger influence on the sample modulus. Generally, the presence of a solid filler increases the Young's modulus of the composites. In the case of the MA-g-wax containing composites (Figure 4.16), the Young's modulus increased with both increasing the sisal and wax contents, and the

differences are also bigger at higher sisal contents. In this case the high modulus could be related to the higher miscibility of MA-g-wax in LDPE, as well as the wax more effectively covering the sisal fibre at low fibre contents.

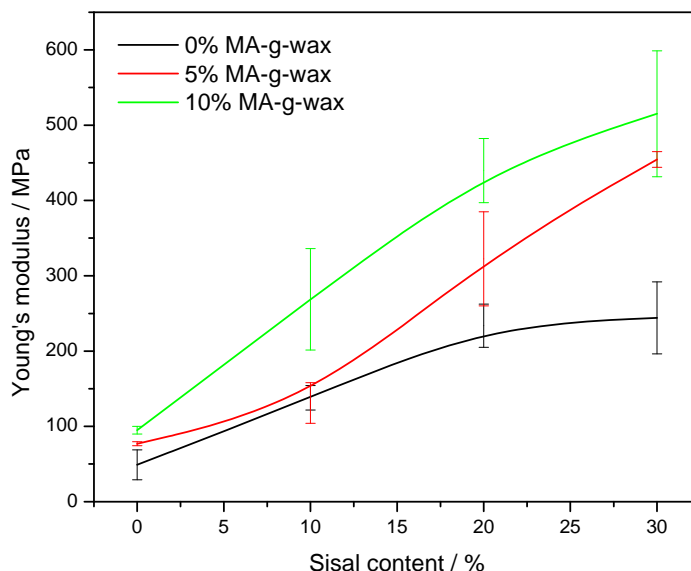


Figure 4.16 Young's modulus as function of sisal content in the LDPE/sisal/MA-g-wax composites

4.5 Dynamic mechanical analysis

The influence of sisal fibre content on the storage modulus (E') and loss modulus (E'') of LDPE is shown in Figures 4.17 and 4.18. The storage modulus of the samples increases with the incorporation of sisal, especially at temperatures above the glass transition of LDPE. This is due to the higher stiffness of sisal compared to that of LDPE. This corresponds to the tensile modulus results of the untreated LDPE-sisal composites. Mohanty *et al.* [15] investigated bio-flour-filled polyolefin composites with different compatibilizing agent type and content. They reported that the tensile and flexural strengths of the jute fibre-reinforced HDPE composites were much higher than those of HDPE. This was associated with the reinforcing effect imparted by the fibres, which was related to a uniform continuous dispersion of the fibres in the polymer [16].

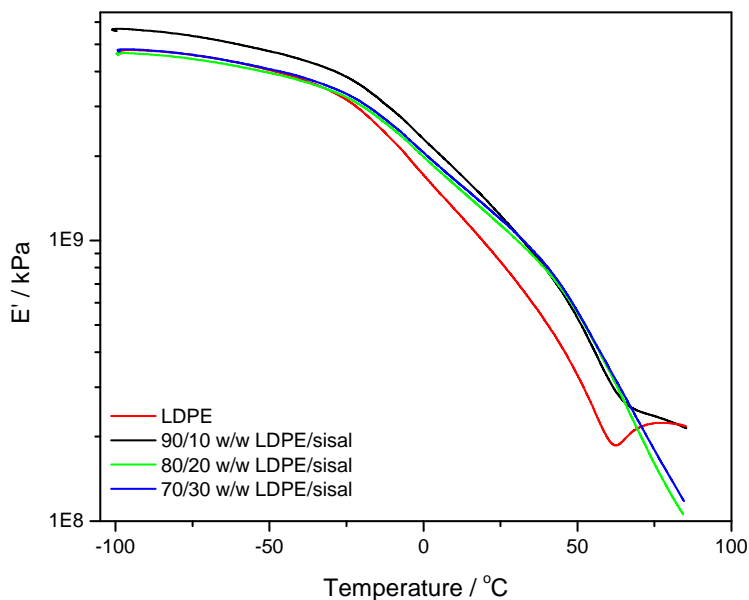


Figure 4.17 DMA storage modulus curves for pure LDPE and LDPE/sisal composites

The composites with 10% sisal content show the highest storage moduli at lower temperatures (-100 to 25 °C), while the moduli of the pure LDPE and composites containing 20 and 30% sisal are very close at lower temperatures. Similar observations were reported by Idicula *et al.* [17], where randomly oriented intimately mixed short banana/sisal hybrid fibre reinforced polyester composites were investigated. The storage moduli of the matrix and the composites were found to be close to each other at low temperatures. They associated this observation with lesser contribution of the fibres towards the stiffness of the material at low temperature. This is in agreement with the results by other authors [18], who further reported that the decrease in storage modulus of the matrix at higher temperature is due to the softening of the matrix, whereas in fibre-filled system it is associated with debonding due to the increased viscoelastic deformation of the matrix at higher temperatures. Different trends were observed by Freire *et al.* [19], where the addition of unmodified fibre to an LDPE matrix led to an increase in the storage modulus values of the composites. There is a general decrease in storage modulus around -25 °C for all the samples which is the β - or glass transition.

Changes in the loss modulus as function of temperature are shown in Figure 4.18. The loss modulus of the pure LDPE shows two well-defined transitions. The first peak at -25 °C corresponds to the β -relaxation, whereas the second peak at around 60 °C may correspond to

the α -relaxation, but may also be the result of the melting of the smallest crystallites. According to Yang *et al.* [20] the relaxation processes observed for PE are labelled as γ , β and α . The γ -relaxation from -50 to -110 °C is caused by small local short-range segmental motion of the amorphous polyethylene and the reorientation of loose chain ends within the crystalline and amorphous fractions. The β -relaxation is the glass transition which corresponds to side chain or pendant group movement in the non-crystalline phase. The α -transition at about 50 °C involves a complex process of molecular mobility within the crystalline phase. Some authors suggest the use of the maximum value of the loss modulus as the glass transition temperature [16,19,21,22]. There is slight shift of the β -relaxation towards higher temperatures (Figure 4.18). This slight increase in the glass transition temperature for the fibre containing samples indicates that the fibre has a slight immobilizing effect on the LDPE chains.

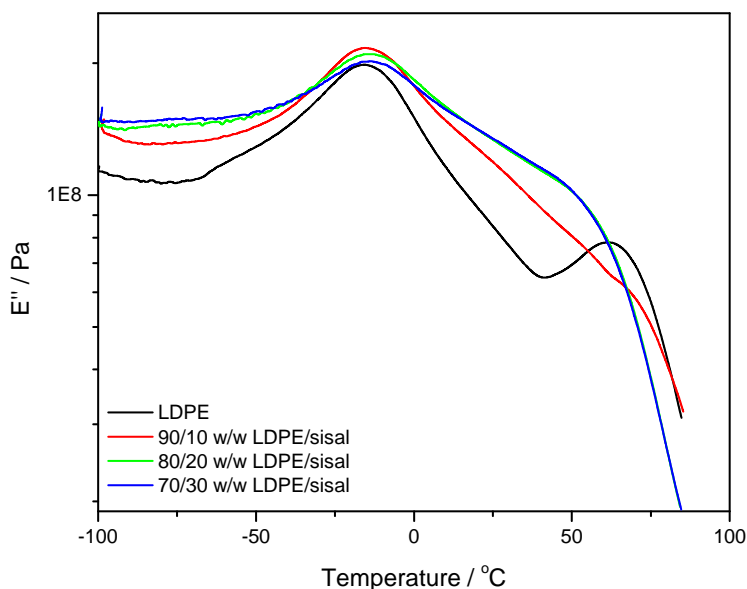


Figure 4.18 DMA loss modulus curves of pure LDPE and LDPE/sisal composites

The storage and loss modulus curves for the pure LDPE and the LDPE/OxWax blends are shown in Figures 4.19 and 4.20. LDPE shows the lowest storage modulus over the whole investigated temperature range (Figure 4.19). This behaviour is in contrast with the observed plasticization effect in the LDPE/OxWax blends as shown by DSC. Plasticization normally reduces the stiffness of a material. Both pure LDPE and the LDPE/OxWax blends show two clearly defined transitions (β - and α -relaxations) which are characteristic of the pure LDPE

(Figure 4.20). The blends show a higher loss modulus compared to pure LDPE. However, the α -relaxation peak for the 10% OxWax containing sample converges with that of pure LDPE. There are no changes observed in the positions of both the β - and α -relaxation peaks.

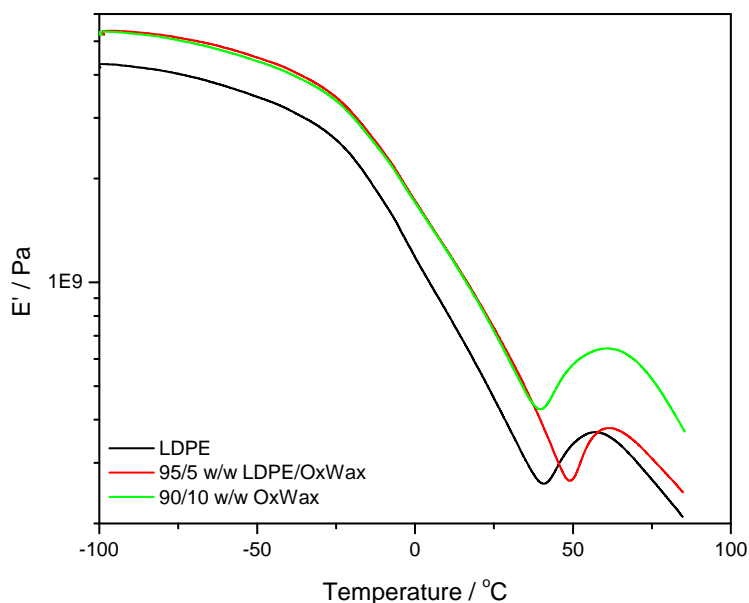


Figure 4.19 DMA storage modulus curves of pure LDPE and LDPE/OxWax blends

Figures 4.21 and 4.22 show the storage and loss modulus of the LDPE/MA-g-wax blends as function of temperature. The pure LDPE shows the lowest storage modulus over the whole investigated temperature range (Figure 4.21). The introduction of MA-g-wax into the LDPE increases the storage modulus, with the highest storage modulus values observed for the 10% wax containing sample. The higher storage modulus may be the consequence of the co-crystallization of MA-g-wax and LDPE chains as observed by DSC (Figure 4.6). The differences are, however, relatively small.

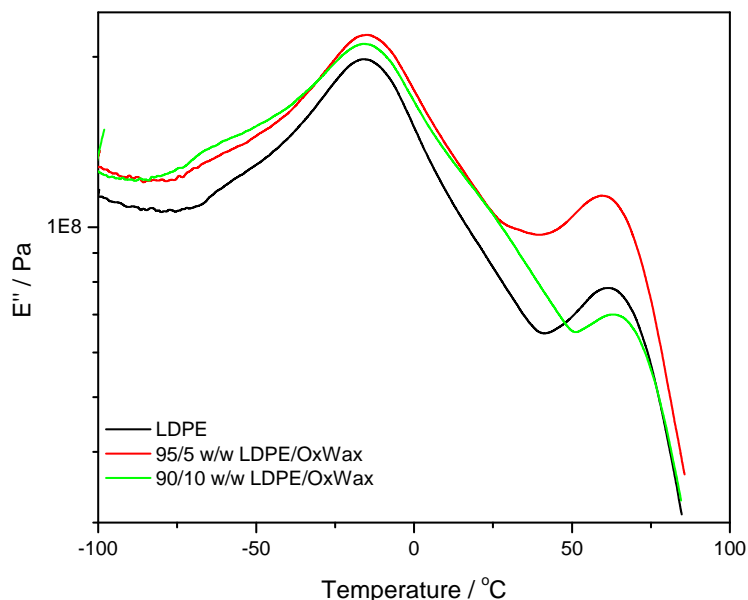


Figure 4.20 DMA loss modulus curves of pure LDPE and LDPE/OxWax blends

Figure 4.22 shows that pure LDPE has the lowest loss modulus throughout the investigated temperature range. These blends also show two well-defined transitions (β - and α -relaxations) that are characteristic of the pure LDPE. There is no observable shift in the position of the β -relaxation peak, but the α -relaxation peak shifted to a higher temperature with increasing wax content. This is probably the result of the higher miscibility of MA-g-wax and LDPE, with the resultant increase in crystallinity.

The storage and loss modulus of the LDPE/sisal/OxWax composites are shown as a function of temperature in Figures 4.23 and 4.24. It can be seen that the pure LDPE shows the lowest storage modulus over the whole investigated temperature range (Figure 4.23). At constant 5% OxWax content with increasing sisal content, there is an increase in storage modulus even though at higher temperatures the 85/10/5 w/w LDPE/sisal/OxWax composites show higher values than the 75/20/5 w/w LDPE/sisal/OxWax composites. The same is observed for the 10% OxWax containing samples. The introduction of both OxWax and sisal increases the loss modulus of the samples (Figure 4.24). The variation of loss modulus with temperature at different OxWax content also shows the same trend as that of storage modulus. All the composite curves show a clear β -relaxation but only pure LDPE and 75/20/5 w/w LDPE/sisal/MA-g-wax composites show a well-defined α -relaxation peak. The presence of

sisal does not seem to have any influence on the glass transition temperatures of the composites.

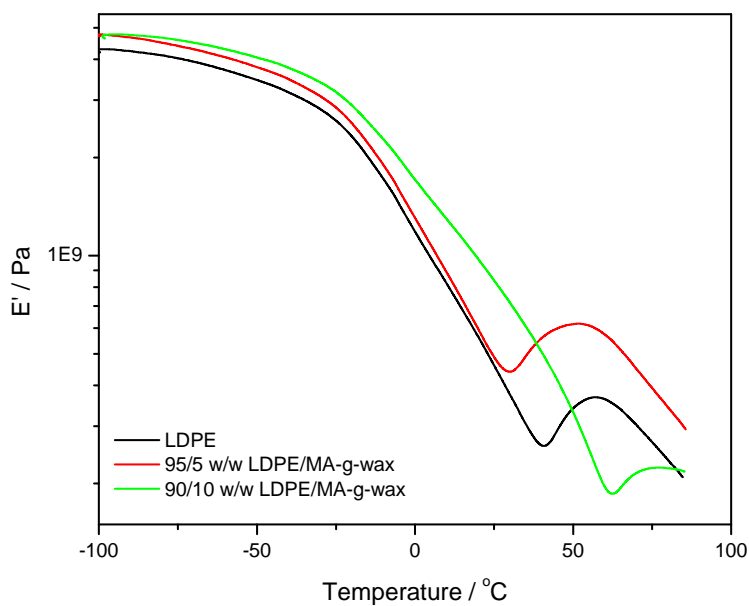


Figure 4.21 DMA storage modulus curves of pure LDPE and LDPE/MA-g-wax blends

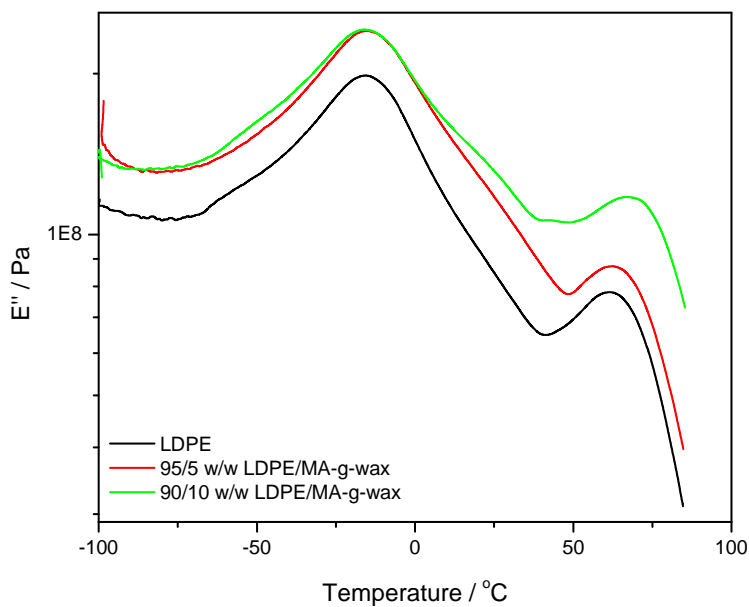


Figure 4.22 DMA loss modulus curves of pure LDPE and LDPE/MA-g-wax blends

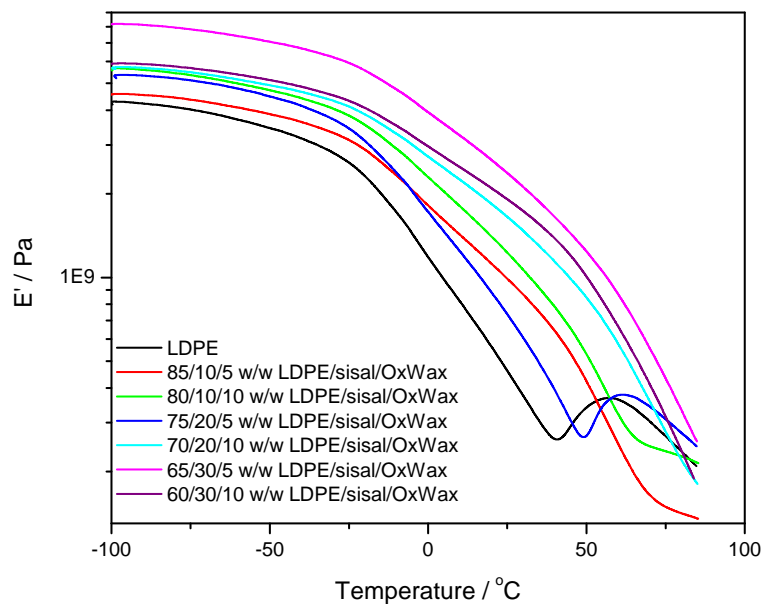


Figure 4.23 DMA storage modulus curves of pure LDPE and LDPE/sisal/OxWax composites

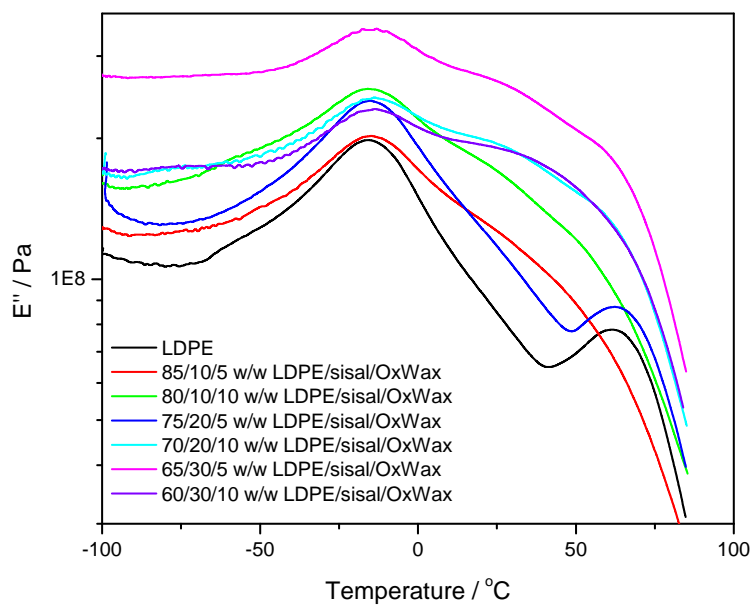


Figure 4.24 DMA loss modulus curves of pure LDPE and LDPE/sisal/OxWax composites

Figures 4.25 and 4.26 show the storage and loss modulus of the LDPE/sisal/MA-g-wax composites as function of temperature. The storage moduli of the 60/30/10, 65/30/5 and 75/20/5 w/w LDPE/sisal/MA-g-wax composites are higher than that of the pure LDPE throughout the investigated temperature range (Figure 4.25). At both 5 and 10% MA-g-wax contents, with increasing sisal content, there is an increase in storage and loss modulus. In Figure 4.26, the loss modulus curves show two transitions, a γ -relaxation at -120°C and a β -relaxation at -25°C . There is a shift of the β -transitions to higher temperatures for both 20 and 30% sisal containing samples. As observed from the DSC and tensile results, at higher fibre content there is not enough MA-g-wax to completely cover the fibres, thus there is probably a stronger interaction between LDPE and sisal.

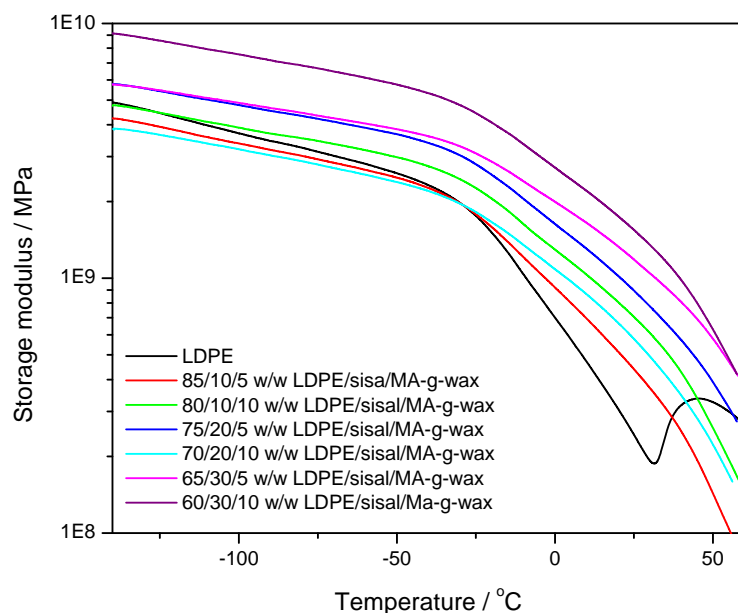


Figure 4.25 DMA storage modulus curves of pure LDPE and LDPE/sisal/Ma-g-wax composites

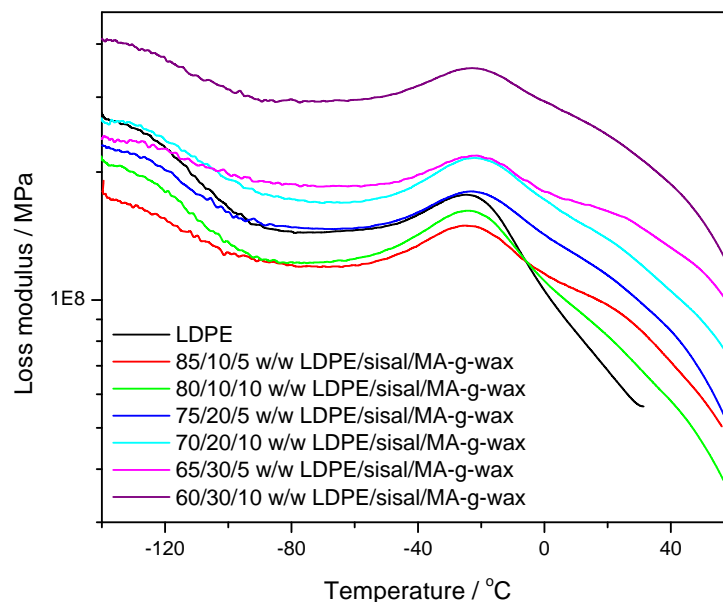


Figure 4.26 DMA loss modulus curves of pure LDPE and LDPE/sisal/MA-g-wax composites

4.6 References

1. G. Sarkhel, A. Choudhury, Dynamic mechanical and thermal properties of PE-EPDM based jute fibre composites. *Journal of Applied Polymer Science* 2008; 108:3442-3453.
2. A.K. Bledzki, A.A. Mamun, O. Faruk. Abaca fibre reinforced PP composites and comparison with jute and flax fibre PP composites. *eXPRESS Polymer Letters* 2007; 1(11):755-762.
3. M. Bengston, M. Le Baillif, K. Oksman. Extrusion and mechanical properties of highly filled cellulose fibre-polypropylene composites. *Composites Part A* 2007 38:1922-1931.
4. A.S. Luyt, I. Krupa. Thermal behaviour of low and high molecular weight paraffin waxes used for designing phase change materials. *Thermochimica Acta* 2008; 467:117-120.

5. S.P. Hlangothi, I. Krupa, V. Djoković, A.S. Luyt. Thermal and mechanical properties of cross-linked and uncross-linked linear low-density polyethylene-wax blends. *Polymer Degradation and Stability* 2003; 79:53-59.
6. Albano, J. González, M. Ichazo, D. Kaiser. Thermal stability of polyolefins and sisal fibre. *Polymer Degradation and Stability* 1999; 66:179-190.
7. M.A. Mokoena, V. Djoković, A.S. Luyt. Composites of linear low density polyethylene and short sisal fibres: the effects of peroxide treatment. *Journal of Materials Science* 2004; 39:3403-3412.
8. I. Krupa, G. Miková, A.S. Luyt. Phase change materials based on low-density polyethylene/paraffin wax blends. *European Polymer Journal* 2007; 43:4695-4705.
9. V. Djoković, T.N. Mtshali, A.S. Luyt. The influence of wax content on the physical properties of low-density polyethylene-wax blends. *Polymer International* 2003; 52:999-1004.
10. F. Vilaseca, A. Valadez-Gonzalez, P.J. Herrera-Franco, M.À. Pélach, J.P. López, P. Mutjé. Biocomposites from abaca strands and polypropylene. Part I: Evaluation of the tensile properties. *Bioresource Technology* 2010; 101:385-395.
11. P. Mutjé, M.E. Vallejos, J. Gironès, F. Vilaseca, A. López, J.P. López, J.A. Méndez. Effect of maleated polypropylene as coupling agent for polypropylene composites reinforced with hemp strands. *Journal of Applied Polymer Science* 2006; 102(1):833-840.
12. J.A. Méndez, F. Vilaseca, M.A. Pélach, J.P. López, L. Berberá, X. Turon, J. Gironès, P. Mutjé. Evaluation of the reinforcing effect of ground wood pulp in the preparation of polypropylene-based composites coupled with maleic anhydride grafted polypropylene. *Journal of Applied Polymer Science* 2007; 105(6):3585-3596.
13. Y. Ruksakulpiwat, N. Suppakarn, W. Sutapun, W. Thomthong. Vetiver-polypropylene composites: Physical and mechanical properties. *Composites Part A* 2007; 38:590-601.
14. S-J. Kim, J-B. Moon, G-H. Kim, C-S. Ha. Mechanical properties of polypropylene/natural fiber composites: comparison of wood fiber and cotton fiber. *Polymer Testing* 2008; 27:801-806.
15. S. Nekkaa, F. Chebira, N. Haddaoui. Effect of fiber treatment on the mechanical and rheological properties of polypropylene/broom fiber *spartium junceum* composites. *Journal of Engineering and Applied Sciences* 2006; 1(3):278-283.

16. S. Mohanty, S.K. Verma, S.K. Nayak. Dynamic mechanical and thermal properties of MAPE treated jute/HDPE composites. *Composites Science and Technology* 2006; 66:538-547.
17. M. Idicula, S.K. Malhorta, K. Joseph, S. Thomas. Dynamic mechanical analysis of random oriented intimately mixed short banana/sisal hybrid fibre reinforced polyester composites. *Composites Science and Technology* 2005; 65:1077-1087.
18. P.V. Joseph, G. Mathew, K. Joseph, G. Groeninckx, S. Thomas. Dynamic mechanical properties of short sisal fibre reinforced polypropylene composites. *Composites Part A* 2003; 34:275-290.
19. C.S.R. Freire, A.J.D. Silvestre, C.P. Neto, A. Gandini, L. Martin, I. Mondragon. Composites based on acylated cellulose fibers and low-density polyethylene: Effect of the fibre content, degree of substitution and fatty acid chain length on final properties. *Composites Science and Technology* 2008; 68:3358-3364.
20. S. Yang, J. Taha-Tijerina, V. Serrato-Diaz, K. Hernandez, K. Lozano. Dynamic mechanical and thermal analysis of aligned vapor grown carbon nanofiber reinforced polyethylene. *Composites Part B* 2007; 38:228-235.
21. W. Qui, T. Endo, T. Hirotsu. Structure and properties of composites of highly crystalline cellulose with polypropylene: Effect of polypropylene molecular weight. *European Polymer Journal* 2006; 42(5):1059-1068.
22. M. Tajvidi, R.H. Falk, J.C. Hermanson, C. Felton. Influence of natural fibers on the phase transitions in high-density polyethylene composites using dynamic mechanical analysis. *The Seventh International Conference on Woodfiber-Plastic Composites* 2003; May 19-20: Monona Terrace Community & Convention Centre, Wisconsin, USA

Chapter 5

Conclusions

5.1 Summary of observations

The purpose of the study was to investigate the effect of functionalized waxes, OxWax and MA-g-wax, as compatibilizers on the morphology and properties LDPE/sisal composites. This was achieved by comparing the uncompatibilized LDPE/sisal composites with the compatibilized LDPE/sisal composites. Composites of different compositions were prepared, and the samples were characterized for their morphology, thermal properties, and mechanical properties using SEM, DSC, TGA, tensile testing and DMA.

5.1.1 Uncompatibilized LDPE/sisal composites

Observations by SEM indicated that for uncompatibilized LDPE/sisal composites there was poor interaction between the matrix and the fibres. The fibres were agglomerated and others pulled out from the matrix when the samples were fractured. As a result, the presence of sisal fibre in LDPE did not influence the melting temperature and enthalpy of LDPE in the composites, and therefore it had a very small effect on the crystallization behaviour of the LDPE. The fibre, however, had a significant effect on the tensile properties of LDPE, especially the elongation at break which was significantly reduced. Both the storage and loss modulus slightly increased over the whole investigated temperature range in the presence of sisal, which indicated some interaction between the LDPE and fibre even in the absence of a compatibilizer.

5.1.2 LDPE/OxWax blends

No significant interaction was observed between LDPE and the OxWax. This was confirmed by both DSC, which showed that these two components were miscible at 5% OxWax content and only partially immiscible at 10% OxWax content, and SEM which showed phase separation between LDPE and OxWax. This led to an initial reduction in the melting temperature of LDPE with no further changes with increasing wax content. There was also no

significant change in the melting enthalpy of the blends compared to that of LDPE. The thermal stability of the blends increased with the introduction of 10% OxWax, which was probably due to (i) the initial protection of wax crystals in the amorphous phase of the polymer by the surrounding thermally stable polymer chains, and (ii) immobilization of free radical chains or volatile degradation products. The presence of OxWax increased the tensile strength of the LDPE matrix, but significantly decreased the elongation at break, probably because of the wax forming crystals in the amorphous phase of the polymer. The presence of 5% OxWax in the blend resulted in a higher modulus compared to the 10% OxWax containing blend, which was attributed to most of the wax being miscible with the polymer at the low wax content, while a large fraction of the wax crystallized separately in the amorphous phase of the polymer at higher wax contents. The storage and loss modulus of the LDPE/OxWax blends were higher than that of pure LDPE, and changes were observed in the positions of both the β - and α -relaxation peaks.

5.1.3 LDPE/MA-g-wax blends

There was a more significant interaction between LDPE and MA-g-wax, as was seen from both the SEM and DSC results. The SEM micrographs revealed that the MA-g-wax was fairly well distributed within the LDPE matrix. This indicated that the two components were more miscible as was confirmed by the DSC results. As a result of the higher miscibility between LDPE and MA-g-wax, the observed melting enthalpy values were lower than the calculated values. Therefore, despite the fact that MA-g-wax was more crystalline than LDPE, the presence of wax lowered the crystallinity of the blends. The 10% MA-g-wax slightly improved the thermal stability of the LDPE, probably because of co-crystallization as seen by DSC, where the less thermally stable wax chains were protected in the thicker lamellae. The presence of MA-g-wax increased the tensile strength of the blends compared to pure LDPE, but the presence of MA-g-wax only slightly decreased the elongation at break values. This was explained as being the result of better interaction between the polymer and the MA-g-wax. The better miscibility between LDPE and the MA-g-wax gave rise to higher modulus values. The presence of MA-g-wax in the LDPE increased both the loss and storage modulus values of the material. There was also no shift in the position of the β -relaxation peak, but the α -relaxation peak shifted to higher temperatures with increasing wax content, which could also be related to the higher miscibility of MA-g-wax and LDPE.

5.1.4 LDPE/sisal/OxWax composites

At low fibre content there was little interaction between LDPE and the fibres as OxWax seemed to completely cover the fibres. The melting peak temperatures of the LDPE/sisal/OxWax composites were lower than that of pure LDPE, probably because of plasticization of the LDPE matrix by the OxWax. The fibres had little influence on the crystallization behaviour of the LDPE, which was also the result of the complete coverage of the fibres by OxWax at lower fibre content. There was an increase in the differences between the observed melting enthalpy and the calculated values as a consequence of more wax crystals in the amorphous phase of the LDPE which probably immobilized the polymer chains and reduced crystallization. The TGA results showed multiple degradation steps. There was a decrease in the tensile strength with increasing sisal fibre content at low fibre contents due to complete coverage of the fibres by the OxWax, but at higher fibre contents the tensile strength increased. This is because there was insufficient OxWax to completely cover the fibres, resulting in stronger interaction between the LDPE matrix and the fibre. As expected, the elongation at break decreased with both increasing wax and fibre contents. Both the storage and loss modulus values of these composites were higher than that of pure LDPE. The presence of sisal and OxWax did not seem to influence the glass transition temperatures of LDPE.

5.1.5 LDPE/sisal/MA-g-wax composites

The SEM results showed that some fibres appeared to adhere to the matrix with no gaps present between the matrix and the fibres. Similar to the OxWax containing composites, there was little interaction between LDPE and the fibres at low fibre contents due to complete coverage of the fibres by the MA-g-wax. The presence of both sisal and MA-g-wax did not have a significant influence on the melting temperature of LDPE in the composites. However, because of better miscibility between LDPE and the MA-g-wax, the experimentally observed melting enthalpy values were lower than the calculated enthalpies for all the investigated MA-g-wax contents. Compared to the OxWax containing composites, the MA-g-wax containing composites had lower thermal stabilities than the neat MA-g-wax. The tensile properties improved with increasing MA-g-wax content. This was the result of better interaction between the MA-g-wax and LDPE, and because the wax concentrated around the fibre, there was stronger interaction between LDPE and the filler. The elongation at break values of the

composites were lower than those of the uncompatibilized composites. The storage modulus of the 60/30/10, 65/30/5 and 75/20/5 w/w LDPE/sisal/MA-g-wax, and the loss modulus of the 60/30/10 w/w LDPE/sisal/MA-g-wax were higher than that of the pure LDPE. There was also an observable shift in the glass transition temperatures for both 20 and 30% sisal containing samples in the presence of MA-g-wax.

5.2 Which wax is the best compatibilizer for the LDPE/sisal composites?

Based on the observations summarized in section 5.1, MA-g-wax may be regarded as the better compatibilizer for the LDPE/sisal composites. A good compatibilizer is anticipated to be miscible with the matrix material as morphology has a significant effect on the polymer properties. Both OxWax and MA-g-wax had an almost similar influence on the tensile properties of the blends, but the tensile properties of the composites improved with increasing MA-g-wax content due to its better miscibility with LDPE, which is not the case with the more immiscible OxWax. The OxWax blends seemed to be thermally more stable than the MA-g-wax blends. The presence of both OxWax and sisal increased the storage and loss modulus of the LDPE in the whole investigated temperature range, but there was no shift in β -transition to indicate whether there was interaction between the matrix and the fibre. In the case of the MA-g-wax containing composites, there was a shift in the β -transitions for the 20 and 30% sisal containing samples, indicating interaction between LDPE and the fibres at higher sisal contents. The lack of interaction between the hydrophobic LDPE and hydrophilic natural fibres compromised some of the important properties of the composite materials.

Acknowledgements

My gratitude and appreciation to my supervisor, Prof A.S. Luyt, for his consistent supervision, guidance, encouragement and patience during all stages of this project.

I am also grateful to Mrs Evangelia Marantos and Dr Nyambeni Luruli, my technical coaches', for following the progress and providing their technical guidance and valuable contributions throughout the research program. Special thanks to my graduate colleagues Mfiso Mngomezulu, Tshwafo Motaung, and Samsom Mohomane, 'Gents' you are the stars. Mr Elias Thole and Leon Bender, for providing a motivating and enthusiastic environment during the many discussions and their helpful feedback and suggestions.

I acknowledge the financial support from NRF and the University of the Free State. I also would like to acknowledge the patience of the Business Support Team in the Polymer Technology Services Centre (Modderfontein), for allowing me to use their time and focus on my studies. The support of the Polymer Research team on the Qwaqwa campus is also acknowledged.

I am grateful to the faculty, staff and my colleagues in the Department of Natural and Agricultural sciences for their assistance in every aspect of my project. I am indebted to my supervisor, the Department of Chemistry, and the University of the Free State for the travel award and financial support throughout my studies.

Finally, above all, special thanks are also extended to Lord Jesus Christ my Sarviour for providing me with the strength and heart to stand throughout this project. For all people will walk every one in the name of their god, and Lefu Piet Nhlapo will walk in the name of the LORD his God for ever and ever, AMEN! (Micah 4:5).

Appendix

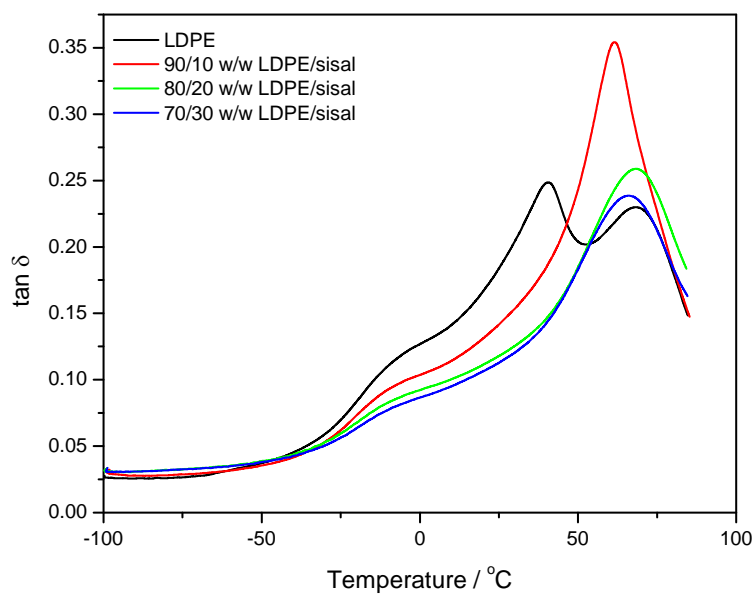


Figure A.1 Damping factor curves of pure LDPE and uncompatibilized LDPE/sisal composites

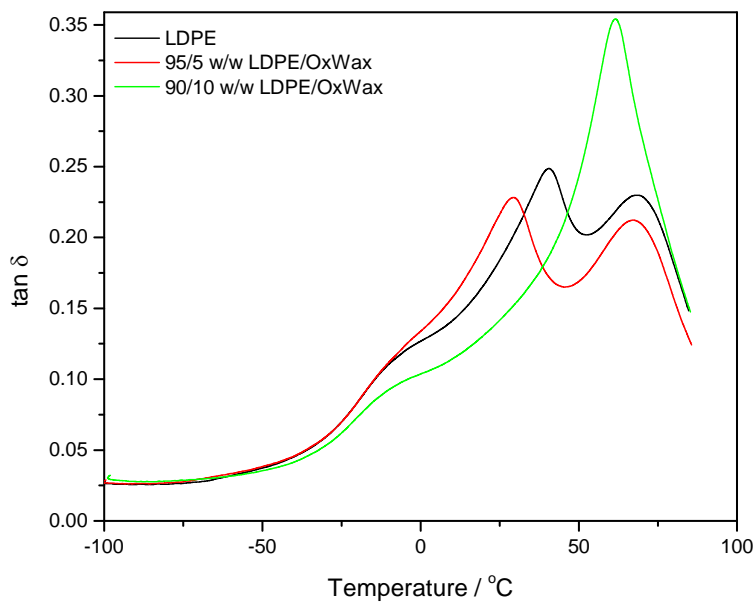


Figure A.2 Damping factor curves of pure LDPE and LDPE/OxWax blends

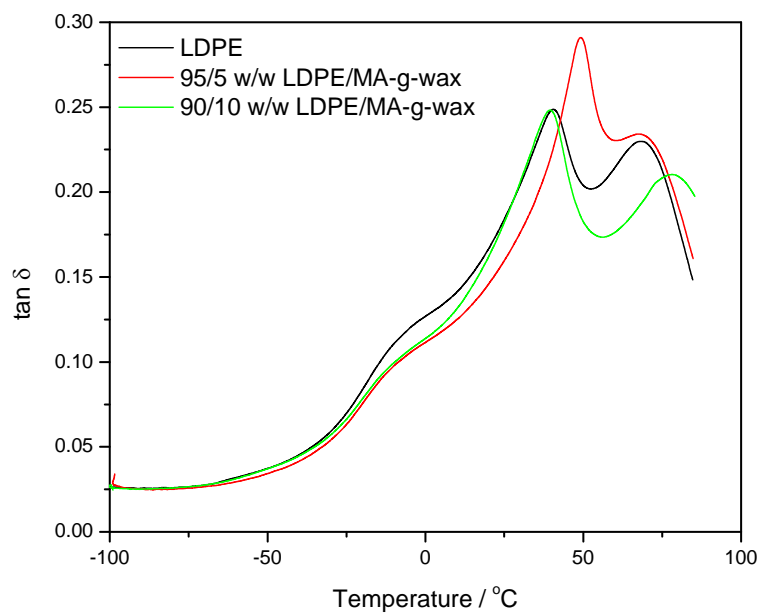


Figure A.3 Damping factor curves of pure LDPE and LDPE/MA-g-wax blends

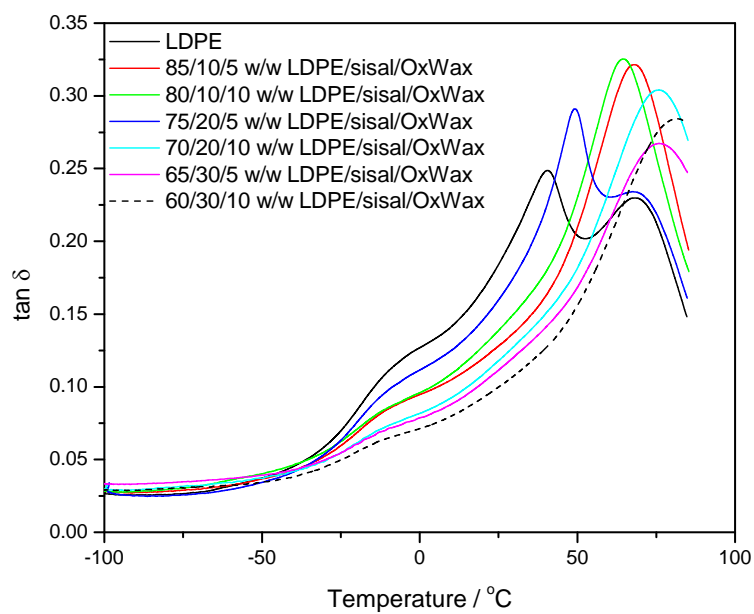


Figure A.4 Damping factor curves of pure LDPE and LDPE/sisal/OxWax composites

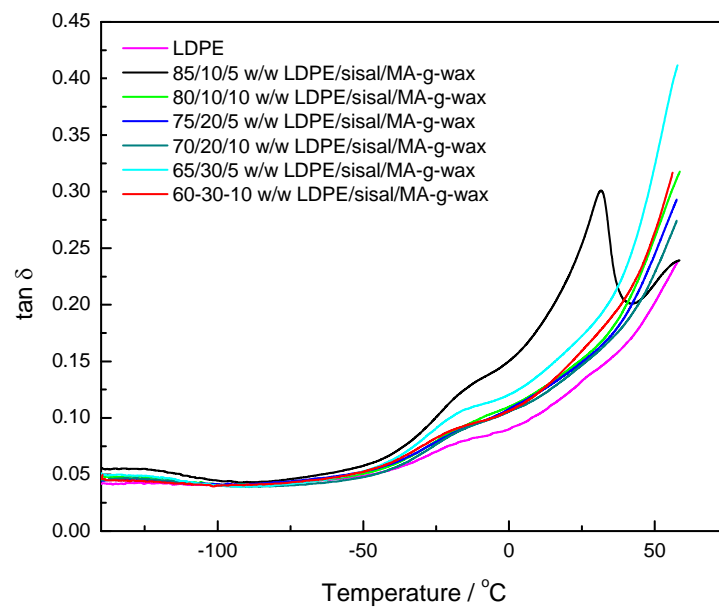


Figure A.5 Damping factor curves for pure LDPE and LDPE/sisal/MA-g-wax composites